

Powering the Future: Unveiling the Secrets of Semiconductor Biointerfaces in Biohybrids for Semiartificial Photosynthesis

Cathal Burns, Elizabeth A Gibson,* Linsey Fuller, and Shafeer Kalathil*



Cite This: *Artif. Photosynth.* 2025, 1, 27–49



Read Online

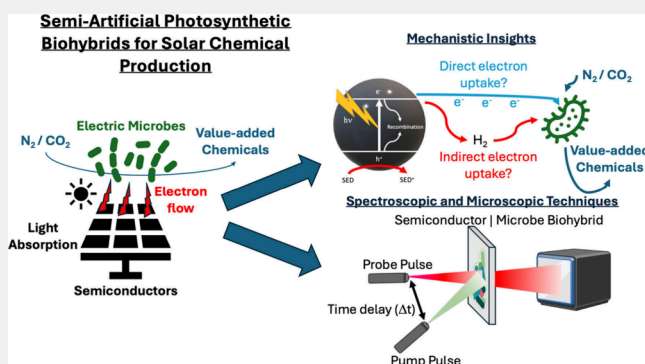
ACCESS |

Metrics & More

Article Recommendations

ABSTRACT: Developing technology for sustainable chemical and fuel production is a key focus of scientific research. Semiartificial photosynthesis is a promising approach, pairing “electric microbes” with artificial light absorbers (semiconductors) to convert N_2 , CO_2 , and water into value-added products using sunlight. Mimicking natural photosynthesis is done with semiconductors acting as electron donors or sinks for microbes. This method enables the production of multicarbon (C_2+) chemicals (e.g., ethanol and caproic acid) and ammonia with high efficiency and selectivity. Despite significant progress, commercial-scale applications remain elusive due to fundamental challenges. This Review covers advances in semiartificial photosynthesis and highlights that there is no clear mechanistic understanding underpinning the production of chemicals using the combination of light, semiconductors, and microbes. Does the mechanism rely on H_2 uptake, do the microbes eat electrons directly from the light absorbers, or is it a combination of both? It focuses on overcoming bottlenecks using advanced spectroscopy, microscopy, and synthetic biology tools to study charge transfer kinetics between microbial cell membranes and semiconductors. Understanding this interaction is crucial for increasing solar-to-chemical (STC) efficiencies, necessary for industrial use. This Review also outlines future research directions and techniques to advance this field, aiming to achieve net-zero climate goals through multidisciplinary efforts.

KEYWORDS: Semiartificial photosynthesis, Biointerface, Microbes, Photocatalysis, Photoelectrocatalysis, Spectroscopy, Microscopy, Solar Chemicals



INTRODUCTION

As society continues to develop, the increasing demand for energy means that new clean energy sources are needed. The overdependence on the burning of fossil fuels as an energy source has resulted in the pollution of the Earth's atmosphere with excess carbon dioxide (CO_2), a well-known greenhouse gas, leading to the gradual warming of the planet. The energy being delivered to the Earth's surface from sunlight is the equivalent of 10000 times more power than is consumed globally. Therefore, developing technologies that can convert solar photons (i.e., visible light) into usable energy such as fuels or electricity is of utmost importance. Plants and photosynthetic bacteria (e.g., cyanobacteria) are the benchmark systems for solar-to-chemical (STC) conversion.

Photosynthetic organisms create a “wireless current” within the photosynthetic membrane upon light absorption. The mechanism of natural photosynthesis is shown in Figure 1. Generating energy dense molecules such as reduced nicotinamide adenine dinucleotide phosphate (NADPH) that can be used in a catalytic cycle known as the Calvin cycle, in which CO_2 is converted to produce biomass and other

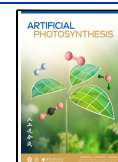
complex organic molecules. The NADPH, which acts as nature's form of H_2 in this reaction, is generated via photon-driven water splitting in photosystems II and I in “the light reaction” and carbon-based fuel; e.g., carbohydrates are produced from the reduction of CO_2 with NADPH in a “dark reaction”. Electrons and holes are separated and transported to opposite ends of the membrane. Holes are used to oxidize water in an oxygen evolution complex composed of manganese and calcium, while photoexcited electrons are used for a reduction reaction to produce NADPH. Biomass and O_2 are produced from CO_2 , H_2O , and sunlight. The solar-to-biomass efficiency of plants is around 1–2% due to poor absorption of sunlight and photodamage, limiting the potential for a biomass-based

Received: May 7, 2024

Revised: August 9, 2024

Accepted: August 13, 2024

Published: August 23, 2024



ACS Publications

© 2024 The Authors. Co-published by
Dalian Institute of Chemical Physics,
CAS, Westlake University, and American
Chemical Society

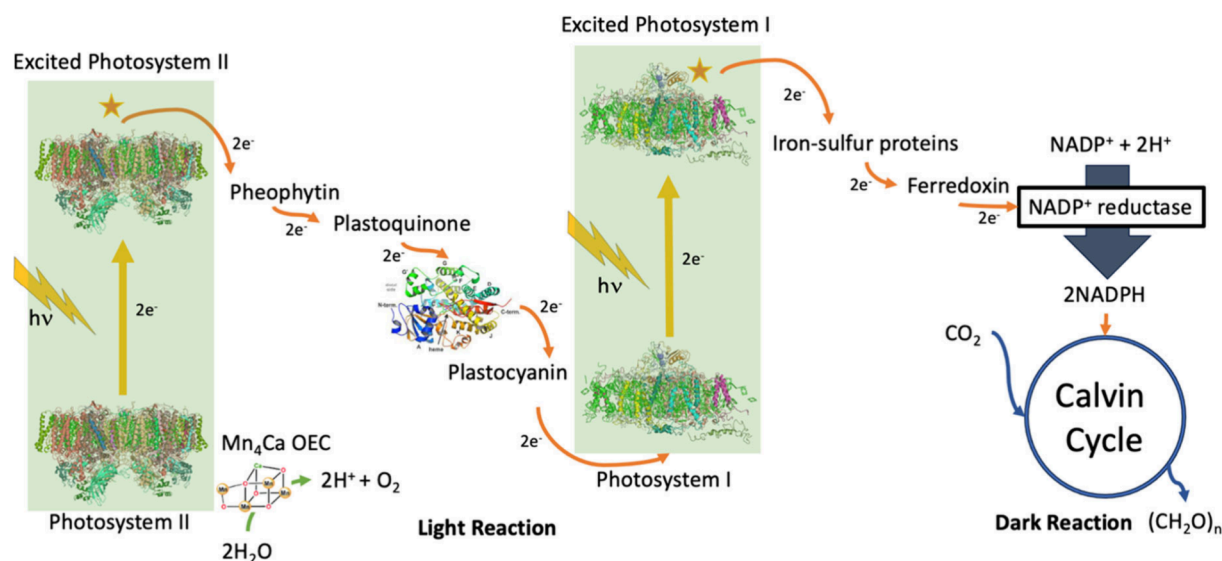


Figure 1. Electron transfer throughout the natural photosynthetic membrane. Photosystems I and II carry out the light reaction, forming reducing equivalents (NADPH). The NADPH is used to convert CO_2 to multicarbon products in the dark reaction.

economy.^{1,2} Therefore, scientists are learning from natural photosynthesis to mimic the elegant biomachinery and trying to beat its efficiency.^{3,4}

For years, artificial photosynthesis⁵ (AP) and photovoltaic^{6–9} (PV) technologies have been studied as alternatives to carbon-heavy chemical and electricity production, respectively. AP uses solar energy to drive chemical reactions and store energy within chemical bonds (“solar fuels”). Artificial photocatalysts can carry out CO_2 reduction to CO with limited ability to produce complex products.^{10,11} Furthermore, direct photochemical and photo(electro)chemical methods of water splitting allow for H_2 production directly from water.^{12,13} Numerous water-splitting systems have been developed, integrating light-absorbing molecules/semiconductors and catalysts to produce H_2 .^{14–19} Even with such a large volume of studies, AP has not been found to match the selectivity of natural photosynthesis, perhaps unsurprisingly, as nature has had billions of years to evolve. Photocatalysis is a wireless system, usually requiring the addition of a sacrificial electron donor (SED) as a necessary evil. Photoelectrocatalysis is a wired system, only using water as an electron donor, making it an elegant and clean system.

The H_2 produced can be used to reduce CO_2 , just as in nature, via a hydrogenation reaction. The benefits of carrying out such a reaction are not only the utilization of waste CO_2 but also the liquid products formed, e.g., formic acid, ethanol, or methanol are much easier to store and transport with current technologies than H_2 gas. Carbon-based fuels can also be used as precursors for the synthesis of other more complex products that are useful in industry. Complex chemical production beyond C_1 chemicals is a considerable challenge kinetically, requiring 10 H^+ and 10 e^- to even achieve ethane (C_2H_6). These proton-coupled electron transfer (PCET) steps are very difficult to achieve using artificial catalysts.²⁰ Hence, an improved method of CO_2 utilization would speed up the attempts to generate fuels at a rate that will compare with fossil fuels.

The overpotentials for CO_2 reduction are also very high, and catalyst surfaces can often be degraded by reduction products. A system capable of total AP, converting both water and CO_2

into organic molecules and O_2 , faces many practical challenges. Chief among these is the multiple PCET steps as previously mentioned. Second to this is the issue of H_2 evolution competing with CO_2 reduction processes in aqueous systems, reducing the Faradaic efficiency and selectivity within these systems. Another challenge is that they are thermodynamically close together, so product selectivity is very difficult, especially vs H_2 evolution. Few examples of light-driven CO_2 reduction systems to C_{2+} chemicals exist.^{21–23} Artificial photocatalytic systems have been reported to convert CO_2 into various products, such as ethanol, acetate, ethene, ethane, and propane.²³ However, the efficiency remains very low due to the complexity of the multiple PCET steps. Low product concentration, poor selectivity, catalyst stability, and high cost often come when using precious metal catalysts like Pt, Ru, and Ir. SAP has great potential to overcome these issues by integrating biological components with artificial light harvesters to produce C_{2+} chemicals from waste CO_2 efficiently and selectively. SAP takes advantage of a “best of both worlds” scenario, where an optimized synthetic light-absorbing material is paired with a microbe/enzyme that can enable light-driven selective catalysis.

Currently, scientists are using four different routes to produce solar fuels, including natural systems, cell hybrids, enzyme hybrids, and artificial systems.²⁴ PV technologies can convert visible light into electrical energy. However, research and development are still required to overcome sunlight intermittency issues in various regions on the planet and the issues with storing the generated electricity. The desired device will need to store and release energy in a manner that can compete with fossil fuels. To compete with carbon-heavy fuel production, 30 TW of fuel/electricity will be needed to maintain human activities by 2050. This equates to covering 0.24% of the earth’s surface with 10% efficient PV and photoelectrocatalytic devices.²⁵

In addition to the well-studied CO_2 conversion technologies, N_2 fixation using SAP is also extremely promising. SAP systems offer several advantages for N_2 fixation over traditional technologies, e.g., the Haber Bosch process, which is highly energy intensive and hugely impactful on the environment.

One key benefit of SAP-driven N_2 fixation is this high energy input is replaced by the efficient conversion of solar energy into reducing equivalents to convert N_2 into NH_3 (a key component in fertilizer) and beyond.

This Review outlines the basic concepts underpinning semiartificial photosynthesis and the techniques that researchers must use to unravel the mechanisms within such systems. This Review begins with a background to the current understanding of SAP microbial systems, outlining the state-of-the-art photocatalytic and photoelectrocatalytic systems for both N_2 and CO_2 fixation. Then, the bottlenecks preventing efficiency from reaching industrial targets are discussed and followed by a discussion on each of the most promising techniques that can be used to study and optimize the biointerface. We finish by outlining the outlook of microbial biohybrids for SAP. The field of semiartificial field has been established over the past decade but is still not well understood mechanistically. There is still a large scope to develop the field to achieve the dream of economically viable solar chemical production. Here, we highlight advances at the interface of physical chemistry, catalysis, biology and material science. This Review also highlights that there is not yet a clear consensus on the mechanism underpinning the production of chemicals using the combination of light, semiconductors, and microbes. Does the mechanism rely on H_2 uptake, do the microbes eat electrons directly from the light absorbers, or is it a combination of both? Through spectroscopy, electrochemistry, and microscopy, the mechanism can be deciphered, allowing researchers to develop systems capable of achieving the necessary efficiency and selectivity for industrial scale-up which would make sustainable feedstock chemicals with the potential to make chemistry a much greener field in the future.

■ CURRENT UNDERSTANDING OF SEMIARTIFICIAL MICROBIAL SYSTEMS

A contemporary approach to overcoming the shortcomings of AP is to incorporate artificial light-harvesting materials (e.g., semiconductors) with enzymes or anaerobic microbes to uptake CO_2 , H_2 , and photogenerated electrons to produce solar fuels/chemicals. This process is called semiartificial photosynthesis (SAP),^{26,27} in which enzyme and microbial cell hybrids show great potential for efficient complex product selectivity in a stable, scalable system capable of utilizing the entirety of the solar spectrum.

In the first SAP systems, biological catalysts (i.e., enzymes) were employed to overcome the synthetic and kinetic challenges found in artificial photosystems. Enzymes are natural catalytic machines consisting of earth-abundant metal centers and cofactors embedded within quaternary proteins.²⁸ Enzymes can carry out PCET, transport of reactants, chemical reactions, and release of products from the active site, reducing the activation energy reactions, therefore, improving the kinetics. This is achieved using steric bulk, electrostatic interactions, and H-bonding, which stabilize intermediates and produce a lower activation energy.²⁹ Semiphotosynthetic enzyme hybrids consist of electroactive/photoactive enzymes paired with light-absorbing semiconductors or molecules to carry out visible light-driven chemical reactions. These enzyme hybrids have been employed to oxidize water, reduce protons, and reduce CO_2 .^{24,30,31} The current bottleneck with enzymatic biohybrids is the stability and longevity of the devices, not to mention the costly and tedious process of identifying and purifying active enzymes. To overcome these issues, microbial

photohybrids can be employed where microbes can function as “living catalysts” with a self-repairing ability and can cope with environmental perturbations. Microbial photohybrids consist of a photoabsorber (e.g., a semiconductor) and anaerobic “electric” microbes³² to use CO_2 , H^+/H_2 , and photogenerated electrons to produce chemical products.³³ Microbial systems have other advantages of being able to utilize as much of the solar spectrum as completely artificial systems, being highly scalable, producing complex carbon products, and giving scientists the capacity to metabolically engineer the microbes to alter product selectivity and efficiency (Table 1 shows a comparison of SAP systems). The current issues of microbial biohybrid systems for SAP involve improving the photosynthetic efficiency, the stability, and the longevity of the systems. Enhancing these factors remains a significant challenge to exceed the efficiencies seen in nature. The optimization of material compatibility is also key to successfully integrating the biological components on the material surface or vice versa, and the toxicity of the chosen materials should be considered. Further optimization is required to find the ideal light intensity, nutrient supply, and temperature required, which will be independent for each system. Lastly, optimized systems will need to be considered in terms of scalability and economic viability using life-cycle assessments. Addressing these issues requires interdisciplinary research and collaboration among many fields.

Photocatalytic Microbial Biohybrids. Figure 2 shows electron transfer across a cell membrane within a photocatalyst-microbial biohybrid for chemical production. Early studies of microbial photobiohybrids were conducted with bacteria containing H_2 ase and N_2 ase enzymes such as *Clostridium butyricum*, *Rhodopseudomonas capsulate*, and *Rhodospirillum rubrum*.^{34,35} These bacteria were coupled with nanoparticles (NPs) of TiO_2 and Bi_2O_3 with methyl viologen (MV) as an electron mediator. In these systems photogenerated electrons were delivered from the conduction band of the semiconductors to the microbes and H_2 evolution was observed.^{34–36} However, these bacteria have limited capabilities as biocatalysts due to their slow growth rate. To overcome this, *Escherichia coli* (*E. coli*) was engineered to express [FeFe]- H_2 ases from *Clostridium acetobutylicum*.^{37,38} The engineered *E. coli* was then added to a mixture of TiO_2 NPs and MV to produce solar H_2 . Mediated systems such as this do however have additional issues such as toxicity to microbes from mediators such as MV as well as the increased cost that results.

The next problem addressed by the community was to fabricate systems capable of utilizing visible light absorption. CdS has been a primary candidate to achieve this in recent years. This time, *E. coli* was engineered to produce H_2 in anaerobic conditions when genetically engineered to express [FeFe]- H_2 ases. CdS NPs were deposited onto the engineered *E. coli* cells.³⁹ Under visible light illumination, more reducing equivalents were produced along the metabolic pathway which resulted in higher H_2 evolution efficiencies. This biohybrid was further improved by encapsulating the CdS-*E. coli* in a silica shell which protected the system from an aerobic atmosphere.⁴⁰ This system showed great stability, continually producing H_2 under illumination for up to 4 days. However, the use of CdS limits the application due to its severe toxicity to microbes.

To fully showcase the catalytic capabilities of microbes, one must look at the process of CO_2 reduction. Microbial

Table 1. Microbial/Semiconductor Biohybrids Comparing Efficiency, Conditions, and Stability^a

semiautificial microbial photohybrid	reaction	conditions	efficiency	stability	ref
<i>Clostridium butyricum</i> /TiO ₂	H ⁺ ⇒ H ₂	illumination: quartz mercury lamp PRK-4 at the bottom of the vessel additives: MV ²⁺ and glucose	16.1 μL H ₂ /3 min	60 min	34
<i>Rhodospseudomonas capsulata</i> /Bi ₂ O ₃	H ⁺ ⇒ H ₂	illumination: 250 W tungsten-halogen lamp additives: MV ²⁺ and starch	590 μL H ₂ /hour	60 min	35
<i>Rhodospseudomonas capsulata</i> /sensitized TiO ₂	H ⁺ ⇒ H ₂	illumination: 50 W Xe lamp (Applied Photophysics, London); the light was filtered through 380 nm filter additives: MV ²⁺ and EDTA	QY = 12.0%	60 min	36
<i>Escherichia coli</i> with [FeFe] hydrogenase expressing genes/TiO ₂	H ⁺ ⇒ H ₂	illumination: 300 W Xe lamp additives: MV ²⁺ and ascorbic acid	QY at 300 nm = 1.57%	5 h	38
<i>Escherichia coli</i> with [NiFe] hydrogenase expressing genes/CdS	H ⁺ ⇒ H ₂	illumination: VL irradiation (200 W cm ⁻²) additives: cysteine	QE = 7.93% and 9.59% (under 470 and 620 nm irradiation, respectively)	3 h	39
<i>Escherichia coli</i> with [NiFe] hydrogenase expressing genes encapsulated in SiO ₂ shells/CdS	H ⁺ ⇒ H ₂	illumination: 350 W Xe lamp additives: MV ²⁺ and ascorbic acid	0.35 μmol/10 ⁸ cells	96 h	40
<i>Methanosarcina barkeri</i> /CdS	CO ₂ ⇒ CH ₄	illumination: 300 W Xe lamp (CEL-HXF300, Ceaulight, Beijing, China) with a 400 nm UV-cut filter additives: cysteine	QE = 0.34%	96 h	44
<i>Morella thermoacetica</i> /CdS-TiO ₂	CO ₂ ⇒ CH ₃ COOH	illumination: 75 W Xe lamp (AM 1.5 G, 5% sun) with 12 h light/12 h dark cycles. additives: Mn-porphyrin and cysteine	80 μmol of CH ₃ COOH in 3.5 days.	3.5 days	46
<i>Morella thermoacetica</i> /Au nanoclusters	CO ₂ ⇒ CH ₃ COOH	illumination: 75 W Xe lamp (Newport) with an AM 1.5 G filter additives: cysteine	QY ~ 3%	7 days	47
<i>Ralstonia eutropha</i> /CdS	CO ₂ ⇒ Carotenoids + PHB + biomass	illumination: fluorescent tubes (80 W m ⁻²) additives: cysteine	PE = 5.98%	8 days	48
<i>Thiobacillus denitrificans</i> /CdS	NO ₃ ⁻ ⇒ N ₂ O	illumination: an LED array composed of 395 ± 5 nm violet LEDs (3.07 ± 0.14 mW cm ⁻²) or a 300 W Xe lamp (CEL-HXF300, Ceaulight, Beijing, China) with a 400 nm UV-cut filter additives: 0.1% sodium lactate and cysteine	N ₂ O, purity in gaseous products was >96.4 ± 0.4%	24 h	49
<i>Morella thermoacetica</i> /PFP/PDI organic semiconductors	CO ₂ ⇒ CH ₃ COOH	illumination: Xe fiber optic lamp (CXE-350, Optpro, China), varied intensities additives: cysteine	QE = 1.6%	3 days	50
<i>Shewanella oneidensis</i> MR-1/CdSe	H ⁺ ⇒ H ₂	illumination: LED (Philips Lumiled Luxeon Star Hex green 700 mA LEDs) at 530 nm (±10 nm), 25 mW ± 5 mW additives: lactic acid	~ 30 μmols H ₂ in 350 h	350 h	54
<i>Cyanobacterium Synechocystis</i> sp. PCC 6803/ITO microarrays	H ₂ O ⇒ H ⁺ + O ₂	illumination: 680 nm, 3 mW cm ⁻² additives: 1 mM DCBQ mediator	mediated photocurrent densities of 245 μA cm ⁻²	7 days	55
<i>Sporomusa ovata</i> Engineered <i>Escherichia coli</i> (to produce acetyl coenzyme A (acetyl-CoA)/SiNWs/TiO ₂ NWs)	CO ₂ ⇒ CH ₃ COOH ⇒ acetyl-CoA	illumination: 300 W Xe lamp with AM 1.5 G filter (Newport, Corp.)	~200 μA cm ⁻² FE ~ 89%	120 h	62
<i>Sporomusa ovata</i> /SiNW cathode coupled to external Si PV	CO ₂ ⇒ CH ₃ COOH	illumination: 300 W Xe lamp with AM 1.5 G filter (Newport, Corp.)	3.6% solar-to-acetate efficiency (0.65 mA cm ⁻²) PE = 10.8%	1 week	64
<i>Ralstonia eutropha</i> /triple junction Si PV coated with CoP/CoPi catalysts	CO ₂ ⇒ PHB + C ₃ ol, C ₄ ol, C ₅ ol	illumination: 1 sun		5 days	69
<i>Sporomusa ovata</i> /Cr ₂ O ₃ /Ru-SrTiO ₃ :La,Rh/ITO/RuO ₂ :BVO ₄ :Mo photo-sheet	CO ₂ ⇒ CH ₃ COOH	illumination: Newport Oriol 67005 solar light simulator (150 W, 100 mW cm ⁻² , AM 1.5 G, λ > 200 nm) with an infrared water filter	STC = 0.7%	15 h	56
<i>Rhodospseudomonas palustris</i> /CdS	N ₂ fixation ⇒ various products	illumination: fluorescent tubes with an 80 W m ⁻² visible light intensity additives: cysteine	PE = 6.73%	9 days	77

Table 1. continued

semiartificial microbial photohybrid	reaction	conditions	efficiency	stability	ref
engineered <i>Xanthobacter autotrophicus</i> external Si PV powered water electrolysis with CoP/CoPi catalysts	$\text{CO}_2 + \text{N}_2 + \text{H}_2 \Rightarrow \text{vitamin B2}$	illumination: 1 sun	$\sim 7 \mu\text{g g}^{-1}$ dry weight cells after 7 days	7 days	79

^aQY/E = quantum yield/efficiency; PE = photosynthetic efficiency; FE = Faradaic efficiency; STC = solar-to-chemical efficiency; PHB = polyhydroxybutyrate; C₃ol = isopropanol; C₄ol = isobutanol; C₅ol = isopentanol.

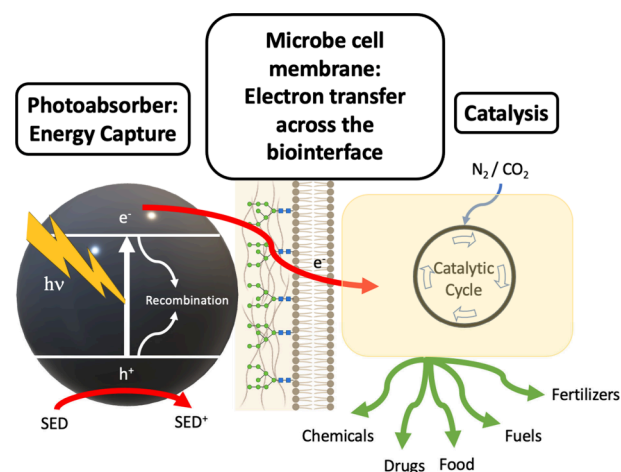


Figure 2. Transfer of photoelectrons across the cell membrane from an artificial light absorber. This represents the key step in improving efficiency in microbial semiartificial photosynthetic systems.

biohybrids can produce complex chemical products owing to their metabolic pathways that have evolved over billions of years. These chemical products are very limited when using synthetic catalysts.⁴¹ Take methane production, for example. Producing methane from CO₂ requires 8 PCET steps. Controlling and coupling PCET steps is notoriously difficult to achieve and failing to do so can result in a range of different products, with very little selectivity control.⁴² Thankfully, biology has evolved to be very effective at carrying out this reaction. The CO₂ to methane reaction can be achieved using methanogenic archaea⁴³ which carry out this reduction as part of an energy conservation mechanism.

Methanosarcina barkeri (*M. barkeri*), a type of anaerobic methanogen, was utilized as the driving force for converting CO₂ into methane,⁴⁴ serving as the catalyst for this transformation. Once again, CdS was deposited onto the microbial surface and the photoelectrons were transferred to intracellular metabolic pathways via H₂ases. These electrons were then used by methanogens to produce methane with a reported quantum efficiency of 0.34%.^{39,40,44} *Moorella thermoacetica* (*M. thermoacetica*), an acetogenic, thermophilic and electrotrophic bacterium has also been hybridized with CdS NPs. In this case, photoelectrons are fed into the Wood-Ljungdahl pathway and used to aid in the conversion of CO₂ into acetate in the presence of cysteine as a sacrificial electron donor (SED).⁴¹ A quantum yield of 2.44% was reported which is even comparable with plants and algae carrying out natural photosynthesis.⁴⁵ Many examples of CdS-microbial biohybrids have been made. However, the toxicity of these NPs remains a huge issue and replacing them with less toxic, more efficient alternatives is at the forefront of the research field.

To make the process more sustainable, Mn(II) phthalocyanine catalysts on TiO₂ were used to regenerate cysteine after it had been oxidized by holes from the valence band of CdS.⁴⁶ Investigations have also taken place to replace CdS with a more biocompatible and less toxic material to absorb visible light. Au nanoclusters have been used to photosensitize *M. thermoacetica*.⁴⁷ It has been established that kinetic drawback stems from transmembrane diffusion of photoelectrons. However, this system was reported to have a quantum yield for acetate production of 2.9% which is again comparable with nature. The process of adding photosensitizing NPs to the

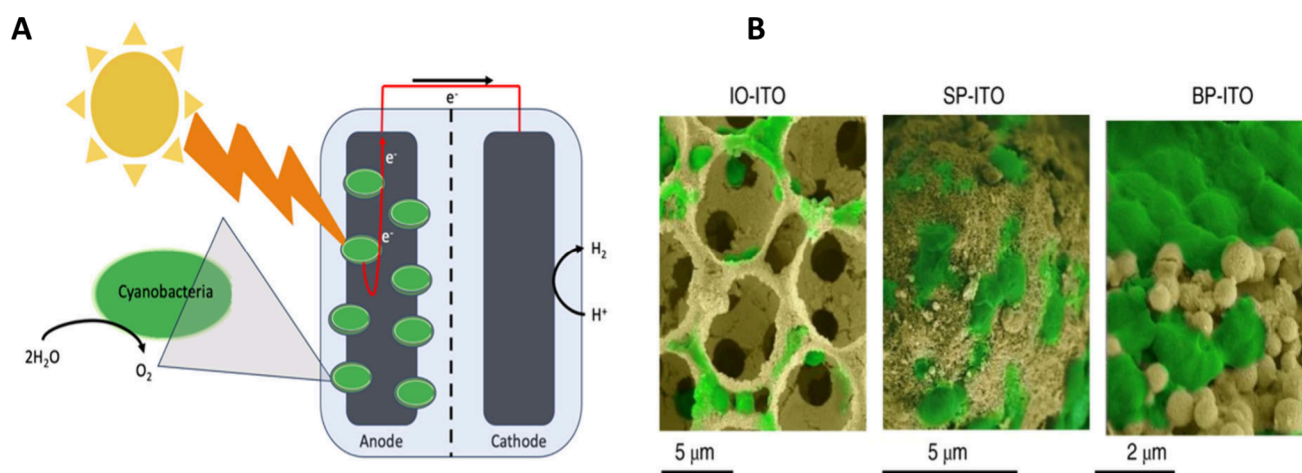


Figure 3. (A) A semiartificial PEC system consisting of a cyanobacteria biohybrid photoanode which can carry out photosynthetic water oxidation. This is wired to a cathode to carry out hydrogen evolution. (B) Representative colorized SEM images of *Synechocystis*-loaded electrodes (top view). Error bars represent the standard error of the mean ($n = 3$). The scaffolds are inverse opal indium tin oxide (IO-ITO), smooth micropillar ITO (SP-ITO), and branched micropillar ITO (BP-ITO). Reproduced with permission from ref 55. Copyright 2022 Springer Nature BV.

surface of bacteria has been well established over recent years, with CdS-*Rhodospseudomonas palustris* being used to fix CO_2 and form biomass, carotenoids, poly(β -hydroxybutyrate) and other complex organic compounds under visible light illumination.⁴⁸ CdS-*Thiobacillus denitrificans* (*T. denitrificans*) biohybrids converted NO_3^- to N_2O under visible light illumination.⁴⁹ CdS has also been replaced with visible light-absorbing organic semiconductors such as a perylene diimide derivative (PDI) and poly(fluorene-co-phenylene) (PFP).⁵⁰ These semiconductors have been reported to be immobilized on the surface of *M. thermoacetica* through supramolecular interactions, such as hydrophilicity and electrostatic interactions, forming a biohybrid with a quantum efficiency of 1.6%. There are numerous examples of dye-sensitized microbial systems producing complex products under visible light and in the presence of a SED.^{51,52} Fumarate to succinate conversion is a useful organic transformation that can be accomplished using whole-cell biohybrids.⁵³ Dye-sensitized (with Eosin Y or pro-flavine) *Shewanella oneidensis* MR-1 (*S. oneidensis*) produced succinate and H_2 gas under visible light illumination and in the presence of methyl viologen (MV) as an electron mediator. Here, MV is toxic and eventually kills bacteria so the development of mediator-free microbial photohybrid systems is needed.

A recent paper published by Edwards et al.⁵⁴ discovered that electron transfer can also be utilized in the opposite direction within microbial photohybrids. This means extracellular electron transfer from microbes to semiconductor NPs. In this case, *S. oneidensis* MR-1 was applied as an electron donor to nanocrystalline CdSe NPs, which were chosen as a highly stable catalyst despite the toxicity issues with Cd and Se salts. This system was used for photocatalytic H_2 evolution. It was reported that electron donation from *S. oneidensis* MR-1 enables H_2 production without any externally applied bias, avoiding the hindrance of the oxidative reaction which is typically sluggish in traditional artificial photocatalytic systems. Monochromatic light illumination with a wavelength of 530 nm excited the CdSe NPs. Holes left on the VB of CdSe were quenched by *S. oneidensis* MR-1. The system reported continuous H_2 generation for 168 h, with the lifetime being hindered by the need to replenish the media with additional

nutrients after this period. Further research is needed to understand this mysterious electron transfer from bacteria to the semiconductors.

Photoelectrocatalysis with Immobilized Microorganisms and Isolated Enzymes. As an alternative to microbial suspensions for photocatalysis, microbes can be immobilized onto a semiconductor surface which can act as a photo-electrode. Immobilisation of microbes can be accomplished via a variety of methods within semiartificial systems. Here, we briefly consider enzyme-based systems also as they form the basis of microbial systems. Simplifying whole-cell systems down to isolated enzymes removes many complications and aids in fundamental understanding.

Chen et al. deposited cyanobacteria via ultrasound-assisted spray coating onto premade IO-ITO electrodes to form biohybrid photoanodes for water oxidation.⁵⁵ Other methods of immobilization have been used, with the most effective being electrodeposition or photodeposition. These methods create a potential difference at the electrode–electrolyte interface which results in the electrostatic attraction of electrotrophic microbes to the material surface.⁵⁶ This electrode can then be wired to a counter electrode and a potentiostat, which can apply an electrical bias if necessary, replacing the need for an SED which makes for a cleaner process. This is known as a photoelectrocatalytic (PEC) system. For example, PEC water-splitting systems can oxidize water at the photoanode and reduce protons at the photocathode without the need for any additional reagents to be consumed in the process. The key step in this process is the electron exchange between the electrode and the microbe.⁵⁷ There are two methods of electron exchange. The first is direct uptake in which microbes accept electrons directly from the semiconductor surface and use the electrons to produce reducing equivalents within the metabolic cycle. The second is indirect uptake in which electron uptake is mediated by H_2 and redox couples. Direct electron uptake has advantages as it negates the need to overcome the solubility and diffusional issues with H_2 and redox couples, respectively. In simple terms, the benefits of the biophotoelectrochemical (BPEC) system over the photocatalytic system resemble the benefits of heterogeneous catalysis vs homogeneous catalysis.

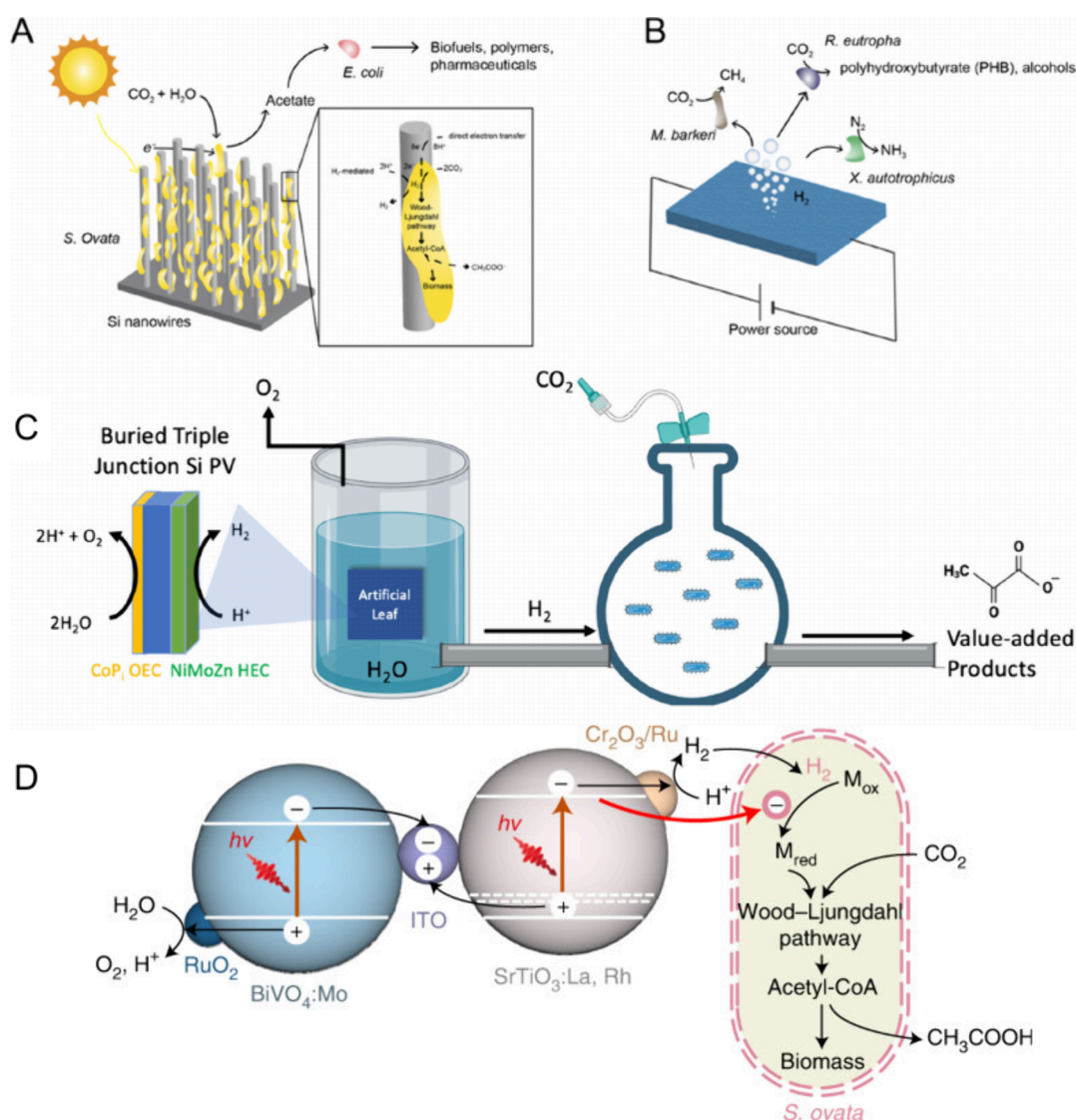


Figure 4. (A) Si NWs interfaced with *S. ovata* for PEC CO_2 -to-acetate production. Reproduced with permission from ref 65. Copyright 2020 Springer Nature BV. (B) Electrocatalytic H_2 producing photocathode paired with various microbes for a variety of catalytic processes. (C) Illustration of Nocera's artificial leaf, which was used to produce a feedstock H_2 to feed *R. eutropha* for production of value-added products. (D) Schematic of a bacteria photocatalyst sheet which was used for bias free CO_2 -acetate conversion. Reproduced with permission from ref 56. Copyright 2022 Springer Nature BV.

Another major benefit of BPEC is the ability to utilize the “electrochemistry toolkit”. In which, electrochemical methods can be used to elucidate electrochemical changes occurring at the biointerface.

Cyanobacteria have been used in tandem with inverse opal indium tin oxide (IO-ITO) electrodes as photoanodes for water oxidation.^{58,59} The cyanobacteria possess the entire photosynthetic apparatus within their cells, making them more stable than PS II biofilms.⁶⁰ A schematic of this system is shown in Figure 3. The mechanism of electron uptake was found to differ between cyanobacteria and PSII biofilms. It is thought that the mechanism by which cyanobacteria take up electrons through intracellular redox mediators under illumination. These mediators then transport electrons to the surface of the semiconductor.⁶¹ However, cyanobacteria lack well-structured membrane networks (e.g., c-type cytochromes) to attach to the electrode which compels them to use soluble chemical mediators to communicate with the electrode, which limits its practical applications.

There are very few reports of microbial biohybrids consisting of nonphotosynthetic microbes grown on semiconductor-based materials. This is because the cells require high surface area electrodes to enable high loading of microbes (biofilms) on the electrode surface without damaging the ability for light to reach the semiconductor.^{62,63} A pioneering example of this system is shown in Figure 4A,B, which was reported by Yang and colleagues, in which an array of Si nanowires was used as an efficient light-absorbing semiconductor and an acetogenic bacterium *Sporomusa ovata* was integrated onto the surface.⁶² The biohybrid photocathode was integrated with a TiO_2 nanowire photoanode for water oxidation. The system represented a bias-free approach to convert CO_2 into acetate and split water simultaneously with an overall STC efficiency of 0.38% over 200 h. The acetate produced was converted into acetyl-CoA which acted as a precursor for a variety of chemical transformations to produce more valuable products.

It has also been reported that improving the biointerface can facilitate acetate production in these systems. Factors such as

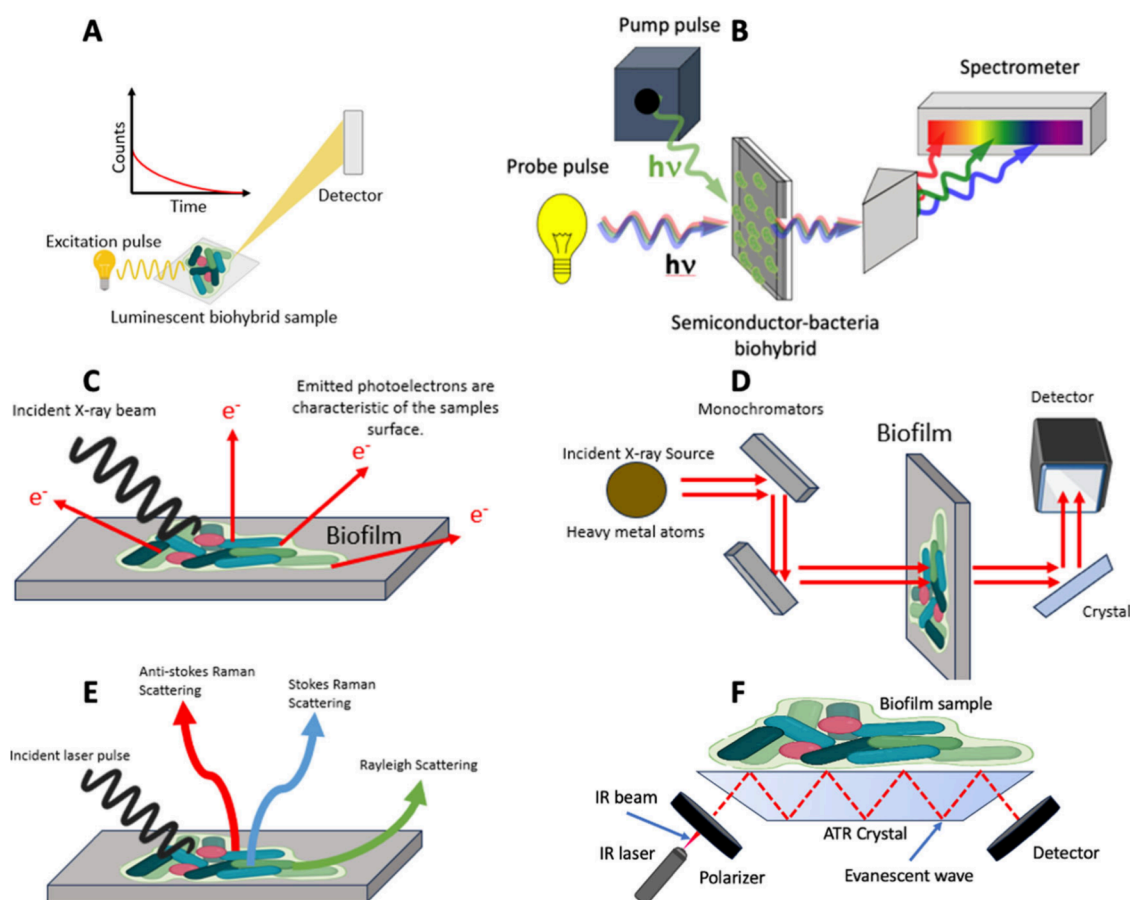


Figure 5. Schematics of various spectroscopy that can be carried out to study microbial-semiconductor biohybrids. (A) Steady-state and time-resolved photoluminescence. (B) Transient absorption spectroscopy. (C) X-ray photoelectron spectroscopy. (D) X-ray absorbance spectroscopy. (E) Raman spectroscopy. (F) Attenuated total reflectance infrared spectroscopy.

increasing the bacterial population in a more controlled pH environment at the interface improved performance to 3.6% STC efficiency when the device was coupled to an external PV device in a photovoltaic-electrochemical (PV-EC) cell.^{64,65} An easier way of fabricating a device with the appropriate morphology and porosity for the most efficient integration of microbes is to use the PV-EC configuration. By coupling porous electrodes with bacteria grown on the surface to an external PV device to power water splitting and CO₂ reduction. These systems can focus on tailoring the electrode structure and take advantage of decades of research that has been established on microbial fuel cells⁶⁶ and recent research on integrating microbes with synthetic materials.^{67,68}

From the research discussed it is obvious that the field of SAP has made huge progress in recent years and is extremely promising. Another very important piece of research to mention is Nocera's artificial leaf (popularly known as "bionic leaf"), which has achieved efficiencies exceeding natural PS.^{20,69,70} In this work, nonprecious metal catalysts carry out PCET, minimizing the activation barrier for water oxidation and proton reduction. The H₂ produced from water splitting powers biosynthesis in carbon-fixing microbes (*Ralstonia eutropha*) to produce liquid fuels via metabolically engineered pathways, as shown in Figure 4C. Another example of recent research has been reported by Reisner et al., which developed a z-scheme photosheet hybridized with *S. ovata*.⁵⁶ Figure 4D shows the hypothesized mechanism of the z-scheme, which resulted in acetate production. In which, there was no need for

a SED, only H₂O (electron donor) and CO₂ were used, making it a clean system. The reported STC (CO₂-acetate) efficiency was 0.7%, representing a benchmark efficiency for a bias-free microbial biohybrid. It is important to note that numerous issues remain within such systems, including the kinetics, light absorption efficiency, and unwanted side reactions.

Microbial Biohybrids for N₂ Fixation. Biological catalysts that produce NH₃, a common ingredient in fertilizer, from N₂ have the potential to replace the conventional NH₃ production method, the Haber-Bosch process. The Haber-Bosch process involves mixing N₂ and H₂ gases at high temperatures and pressures, which is highly energy extensive.^{71–74} The Haber-Bosch process has previously been described as the most important innovation of the 20th century and has been utilized globally on an industrial scale for over a century.⁷⁵ However, it is now time to find a more sustainable method of NH₃ production. Electrochemical N₂ reduction using artificial catalysts has been reported but efficiency remains low due to the difficulty in reducing extremely stable N₂ molecules.⁷⁶ Microbial biohybrids can similarly be used to convert N₂ into NH₃, representing a promising, green method for NH₃ production. N₂-fixing microbes offer access to highly evolved metabolic pathways that can produce NH₃ at much greater efficiencies than artificial catalysts.

Wang et al. used a combination of CdS NPs and the photoheterotrophic bacteria (*R. palustris*)⁷⁷ for the photo-

catalytic conversion of N_2 to ammonia. Photoexcitation of the CdS NPs was found to greatly enhance N_2 fixation and biomass production increased by 153%. Lu et al. designed a photoelectrode-based biohybrid system which consisted of silicon microarrays with *X. autotrophicus* and *B. japonicum* producing biomass and NH_3 . The N_2 reduction rate was reported to be 2× greater than under dark conditions.⁷⁸ The design of a microarray allows the O_2 gradient of the system to be controlled allowing for NH_3 to be produced by anaerobic microbes using only clean electricity as an energy source. This proof-of-concept study opens the door for researchers to improve this technology to make NH_3 production from biohybrid systems a sustainable and commercially viable approach.

Recent research by Nocera et al. utilized an engineered strain of *Xanthobacter autotrophicus*, which was fed green H_2 , CO_2 , and N_2 .^{79,80} The H_2 was generated using a PEC water-splitting device, and a step further than ammonia production was achieved. It was possible to overproduce vitamin B2. Plasmids and promoters were identified that can be directly involved in the production of vitamin B2, with a 15× increase in production reported in comparison with the wild-type strain.

However, there are still numerous limitations to these systems that will need to be understood and overcome before an increase in STC efficiency can be seen, to make the technology able to compete with carbon-heavy energy production. Strategies are required to elucidate the complex mechanism at the biointerface to couple the incoming and outgoing flux. Also, considerations are needed to understand the movement of electron carriers, needing to side-step the biological membrane barriers and avoid alternative charge-transfer pathways that could result in charge recombination.⁸¹

■ METHODS TO OVERCOME THE CURRENT BOTTLENECKS OF SEMIARTIFICIAL SYSTEMS

There are various techniques that can be used to develop an understanding of charge transport between semiconductors and bacteria. Spectroscopy techniques include ultrafast transient absorption spectroscopy (TAS), attenuated total reflection infrared spectroscopy (ATR-IR), time-resolved and steady-state photoluminescence spectroscopy (PL), UV–visible absorption spectroscopy, and X-ray photoelectron spectroscopy (XPS). The combined application of these techniques will provide a well-rounded picture of what is happening at the interface. It is possible to measure the kinetics of the reactions that occur following light absorption on as short as femtosecond timescales, enabling rapid energy or electron transfer processes to be tracked.

Another equally important aspect of optimizing the semiconductor biointerface is to study the morphology of biohybrid systems. This can be done using microscopy. Transmission electron microscopy (TEM) and scanning electron microscopy (SEM) allow the structure of the systems to be imaged down to the nanometer scale. In tandem with microscopy, X-ray diffraction can be used to analyze the elemental components of the semiconductors and microbes. Compiling a wide variety of these techniques is the most reliable strategy to interpret the charge transfer mechanism and the factors that can improve or hinder the process.

The challenge of seamlessly integrating synthetic light-absorbing materials with biological catalysts can be overcome with various spectroscopic techniques. Here we have identified and evaluated the most common and useful techniques for

unravelling the interactions at the biointerface, illustrated in Figure 5. The techniques discussed in the forthcoming sections are used as a standard to analyze artificial thermal and photocatalytic systems. However, they have not yet been sufficiently used to study photobiohybrid systems which may be due to the complexity of the systems. Heterogeneous biohybrid systems present specific difficulties when measuring. For example, working in water presents difficulties when using infrared techniques. Also, most microbes used in BPEC systems function under anaerobic conditions. Carrying out certain spectroscopy techniques within strict O_2 -free environments presents engineering and experimental design challenges. Electrochemistry is another powerful technique for evaluating the efficiency of biohybrid systems. Key concepts in electrochemistry can allow researchers to accurately study the selectivity and efficiency of (photo)electrochemical systems. Current densities and photocurrent densities (the quantity of current travelling per unit area e.g. $mA\ cm^{-2}$) are important figures of merit. Faradaic efficiencies (FE) can be used to benchmark the system's selectivity toward a specific product within an electrochemical process. FE is defined as the amount of product relative to the charge passed and is given as a percentage. Finally, another useful term to note is the 'overpotential' observed for a given system which is the potential difference between a thermodynamic reduction potential of a process and the experimentally observed redox potential. These parameters are important to determine the efficiency of the photoelectrochemical cell.

Steady-State and Time-Resolved Photoluminescence Spectroscopy. Steady-state and time-resolved PL are powerful techniques that can be applied to study microbial biohybrids. PL can provide insight into energy transfer within these systems, the behavior of excitons (electron–hole pairs), and the recombination of charge carriers.⁸² Steady-state PL measures the emission of light from a material under excitation. Emission spectra can provide insights into electronic energy levels, charge transfer states, and optical properties. Alternatively, time-resolved PL provides a detailed understanding of excited state lifetimes and charge transfer dynamics by measuring the decay of the excited state over time. The samples are excited with a short pulse of laser light (often on the nanosecond time scale). The emission intensity is then measured at a fixed wavelength as a function of time. In the context of microbial biohybrids, PL can be used to study the emission properties of light-harvesting materials and understand their interaction with microbes. Factors such as charge separation and recombination can be studied and optimized which can improve the STC conversion efficiencies of the biohybrids. PL is a common technique for evaluating and optimizing PV devices and photocatalysts with factors such as excited-state lifetime (τ) and quantum yield (ϕ) strongly correlating to the calculated solar-to-fuel efficiency reported. Despite this, it has been rarely used to evaluate microbial biohybrids in SAP. This may be due to technical problems such as the difficulties in system stability and complex system integration. An obvious disadvantage of using PL on SAP systems is that if the light-absorbing semiconductor is not luminescent then PL cannot be used. In PL spectroscopy, radiative transitions of any luminescent material or molecule can be calculated using eq 1. Nonradiative emission can also occur and can be calculated using eq 2. k_r remains nearly constant for any chromophore. Therefore, to increase the luminescence quantum yield, a decrease in k_{nr}

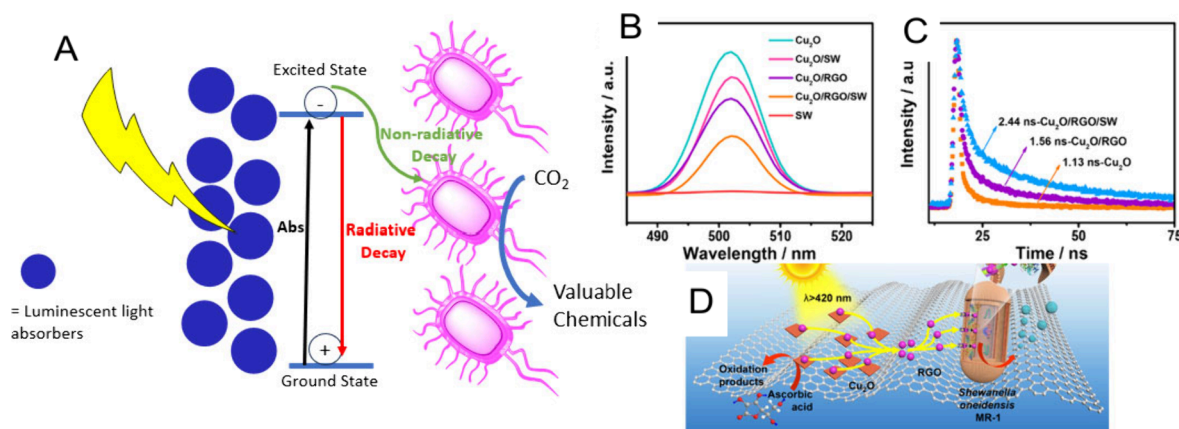


Figure 6. (A) Illustration of photoluminescence along with a typical excited-state lifetime decay spectrum. (B, C) Steady-state and time-resolved PL spectra of $\text{Cu}_2\text{O}/\text{RGO}/S. \text{oneidensis}$ samples, showing electron transfer from material to bacteria. (D) Schematic of electron transfer throughout the $\text{Cu}_2\text{O}/\text{RGO}/S. \text{oneidensis}$ system. Reproduced with permission from ref 83. Copyright 2020 American Chemical Society.

must occur which could be attributed to the formation of additional electronic pathways, e.g., ET from semiconductor conduction band to an electron acceptor within the microbe. As shown in eqs 1–4. Using PL spectroscopy will prove to be a hugely important tool in evaluating and improving microbial SAP systems.

$$k_r = \frac{\phi}{\tau} \quad (1)$$

$$k_{nr} = \frac{1 - \phi}{\tau} \quad (2)$$

$$\phi = \frac{k_r}{k_r + k_{nr}} \quad (3)$$

$$\tau = \frac{1}{k_r + k_{nr}} \quad (4)$$

In a study of Cu_2O , reduced graphene oxide (RGO), and *S. oneidensis* carried out by Shen et al. to boost photocatalytic H_2 production, the PL showed electron transfer upon excitation of Cu_2O to RGO to *S. oneidensis* in the form of PL intensity quenching, shown in Figure 6B–D.⁸³ The lifetimes of the $\text{Cu}_2\text{O}/\text{RGO}$ was 1.58 ns which increased to 2.44 ns upon the addition of bacteria ($\text{Cu}_2\text{O}/\text{RGO}/S. \text{oneidensis}$). The lifetimes for state-of-the-art abiotic photocatalysis measured using TR-PL can range from fs to ns. The lifetime of biohybrid systems is slower than the lifetimes reported for state-of-the-art abiotic photocatalytic systems. The authors conclude that this is unsurprising as within the microbial system the rate-determining steps (electron transfer across membranes and metabolic pathways) are much slower than in artificial systems.

Luo et al. also utilized *S. oneidensis* for H_2 evolution. In this case, bacteria were sensitized with $\text{CuInS}_2/\text{ZnS}$ quantum dots (QDs).⁸⁴ Photocatalytic H_2 evolution was found to be 8.6× higher for the biohybrid than the sole QD system and the biohybrid was found to produce H_2 for over 45 h. PL spectroscopy was used to study electron transfer at the biointerface. PL intensity of QD/*S. oneidensis* with double deletion of hydrogenase enzymes showed a small decrease. However, a much larger quenching of emission was observed in the sample with hydrogenase, suggesting that hydrogenases play a significant role in electron uptake within these systems. TR-PL showed that the excited state lifetime of the QD's was

266 ns which decreased to 62 ns upon the addition of *S. oneidensis* indicating that electron or energy transfer was occurring to the microbe. Additionally, transient absorption spectroscopy (TAS) was carried out to investigate the electron transfer mechanism between hydrogenase and QD. The theory of TAS is explained later in this review. The bleach recovery of the biohybrid was found to be faster than the QDs alone, 14 and 42 ps, respectively. This confirmed the hypothesis that the hydrogenase was able to trap photoexcited electrons. Interestingly, the kinetics of the biohybrid differed from the kinetics between the same QDs and molecular Co catalysts where the electron transfer rate was found to be > 8 ns for the QDs and around 1–2 ns upon the addition of the catalysts.⁸⁵

Still, a huge unanswered question is whether all photons that have been absorbed by an artificial light absorber be transferred efficiently across the biointerface to increase STC efficiencies. PL spectroscopy can provide key insights into the mechanism as shown above through quantifying quantum yields and excited state lifetimes. A report by Guan et al. showed that interfacing *Xanthobacter autotrophicus* (a N_2 and CO_2 fixing bacterium) with CdTe NPs could drive both CO_2 and N_2 fixation using visible light with high quantum efficiencies ($47.2\% \pm 7.3\%$ and $7.1\% \pm 1.1\%$, respectively).⁸⁶ PL spectroscopy was utilized to track electron transfer from the emissive CdTe NPs to *X. autotrophicus*. These high quantum efficiencies are on par with the biochemical maximum which can be calculated from the stoichiometry of biochemical pathways. CdTe QDs were reported to be photophysically stable and had an excited state lifetime of 49.4 ± 0.5 ns. The authors then added cysteine and *Xanthobacter autotrophicus* to two separate dispersions of CdTe QDs. The PL intensity was shown to decrease by 6% upon the addition of cysteine and by 43% upon the addition of *X. autotrophicus*, suggesting that electron/energy transfer is occurring. The average lifetimes of the samples were found to be 49.6 ± 0.5 ns and 48.3 ± 0.5 ns, respectively. A sample containing cysteine, *X. autotrophicus*, and CdTe QDs was also tested. This displayed a similar emission intensity to the cysteine-only sample, but the emission intensity decreased to nil after only 8 h (as the QD's attached to the microbe surface) and the lifetime was shown to be much shorter than previous samples (4.4 ± 0.3 ns after 24 h). The authors were able to rule out aggregation of the QDs as the source of luminescence quenching through abiotic control experiments with aggregated CdTe particles. It

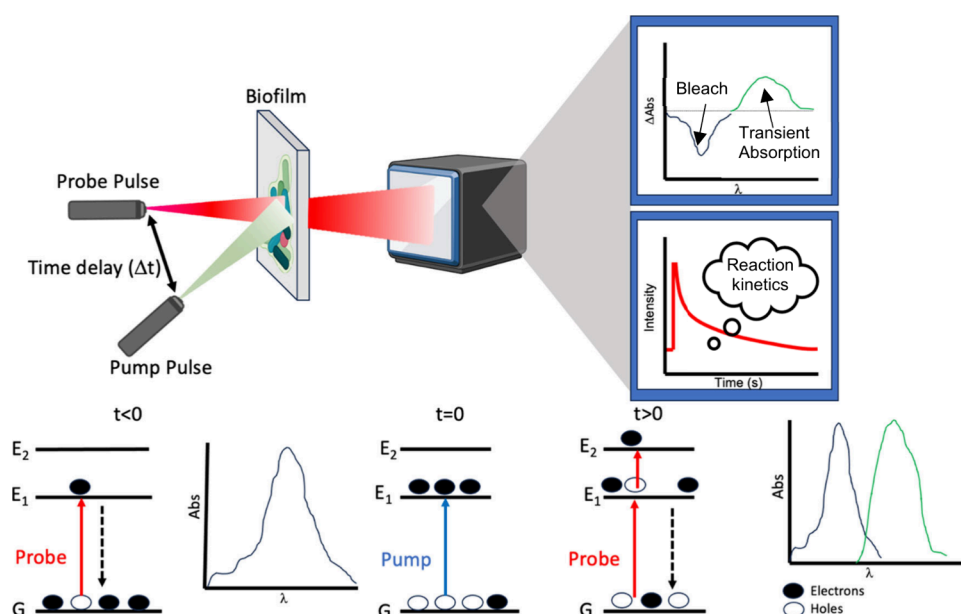


Figure 7. Model pump-probe system with beams and a detector measuring attenuated light which produces a difference in absorbance or transmission spectrum. The difference spectrum (shown on the top right) represents the reagents (bleach) and the products (transient absorption). Then, the decay profile of the absorption/ transmission bands decay over time which can be used to obtain the lifetimes of different states and this can be converted to a rate constant. The base of the figure shows how the pump probe technique generates the initial excited state (E_1) and how the technique promotes electrons to a higher energy state (E_2), which allows the measurement to take place.

was therefore concluded that the combination of cysteine, microbes, and QDs led to fast charge transfer between excited QDs and microbes. The rate of electron transfer was calculated to be $2.1 \times 10^8 \text{ s}^{-1}$, which was much faster than the rate of radiative and nonradiative decay ($k_r = 1.2 \times 10^7 \text{ s}^{-1}$, $k_{nr} = 8 \times 10^6 \text{ s}^{-1}$), and the rate of quenching from cysteine molecules ($k_Q = 1 \times 10^6 \text{ s}^{-1}$). It seems from the results reported that the introduction of CdTe QDs can alter the microbe's metabolic pathway. A preference for CO_2 and N_2 fixation is observed and a decrease in the rate of synthesis of ATP-demanding molecules was also observed, decreasing these reactions increases the observed quantum yield. This metabolic response was attributed to the delivery of reducing equivalents to membrane-bound enzymes as the QD/microbe contacts are nondiffusive therefore reducing equivalents were delivered preferentially to these enzymes. This work represents a great example of how interdisciplinary research, such as the use of PL spectroscopy and synthetic biology, can answer key questions within the field.

Transient Absorption Spectroscopy. Transient absorption spectroscopy (TAS) is possibly the most useful tool when investigating the dynamics of charge transfer across the biointerface as the kinetics of electron transfer can be directly extracted. In a typical TAS experiment, the sample is excited with a “pump” pulse, which promotes electrons into an excited state. This is followed by a “probe” pulse which arrives at the sample after a controlled time delay. Absorbance measurements are made at various time delays. By varying the time delay and plotting change in absorbance spectra the evolution of transient species can be tracked (Figure 7). The temporal resolution of TAS is dependent on the duration of the laser pulses. Using femtosecond lasers provides an ultrafast time resolution, which enables very short-lived transient species to be observed.^{87–89} Another advantage of using TAS on biohybrid samples is that biological samples are often tagged with fluorescent proteins or molecules to image or track

processes. TAS can gain insights into nonfluorescent biological samples without any additional additives.

Challenges with TAS of biohybrid samples include noisy spectra that may be produced from heterogeneous biological samples, interpretation challenges with various complex processes potentially occurring simultaneously as often there are many overlapping chromophores present in the same sample, and the sensitivity of living biohybrid samples being exposed to concentrated laser pulses. Factors such as solvent effects, spatial proximity, reorganization energies, and H-bonding can all alter the kinetics observed in TAS.

TAS was used to study the mechanism of semiartificial photosynthetic acetate production from CO_2 in a CdS-*M. thermoacetica* biohybrid.⁸⁷ The excited state decay kinetics of the CdS were studied with and without microbes. In samples including CdS and *M. thermoacetica*, a transient bleach was observed in the TAS spectrum between 440 and 490 nm which was attributed to electron transfer from the conduction band of CdS to *M. thermoacetica*. The bleaching was not observed in the samples of *M. thermoacetica* alone. TAS of CdS QDs without bacteria showed much slower excited state decay kinetics than the biohybrid sample, strongly indicating electron transfer from semiconductor to microbe (Figure 8).^{87,88} *M. thermoacetica* that was incubated in H_2 presented even more rapid decay than the glucose analogue, which suggested that hydrogenase enzymes were crucial in the electron-uptake mechanism. The TAS was fitted to a triexponential decay function, which showed the presence of 3 different lifetimes: a fast component (2–10 ps), a 20–80 ps component and a several hundred ps component. This unsurprisingly indicated multiple processes occurring within the biohybrid system. Electron relaxation occurs in the fs range for Cd chalcogenide QDs, hence, this was discounted from contributing to the kinetics.⁹⁰ Previous reports of CdS QDs and FeFe hydrogenases were found to possess lifetimes of $\sim 100 \text{ ns}$, much longer than with *M. thermoacetica*.⁹¹ The difference was

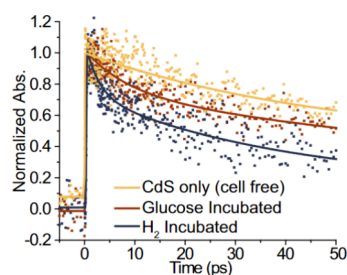


Figure 8. TA spectroscopy of *M. thermoacetica* - CdS showing TA plots of CdS only (cell-free), 24 h glucose incubated, and 24 h H₂ incubated. Reproduced with permission from ref 87. Copyright 2016 PNAS.

hypothesized to be due to the presence of surface ligands on these CdS QDs hindering charge transfer processes, which are not present in the CdS-*M. thermoacetica*. This comparison demonstrates the complexity of working with complex biological systems with multiple interactions occurring simultaneously. It was further thought that a molecular carrier may also be responsible for transferring charge to the hydrogenase enzymes. Hydrogenase enzyme activity was correlated by varying the time of H₂ incubation. Both fast lifetimes shortened with increasing hydrogenase activity, suggesting the increased presence of hydrogenase acceptors and increasing electron transfer kinetics. CO was also used to inhibit the active site of the hydrogenase which did not alter the observed kinetics. This suggests electron transfer does not occur through the active site, which is consistent with previous research into hydrogenase enzymes.⁹¹

A recent report by Baikie et al.⁹² applied ultrafast (picosecond) TAS to measure electron extraction throughout the photosynthetic membrane of live cyanobacterial cells and with isolated PSI/ PSII in the presence of an electron mediator such as MV or 2,6-dichloro-1,4-benzoquinone (DCBQ). An electron mediator is a compound capable of facilitating electron transfer between redox-active components, e.g., a

microbe or an enzyme and another redox-active substance or an electrode. The results shown are very interesting and challenge the previously established models of natural photosynthetic systems (Figure 9). The results suggest that the mediators (MV and DCBQ) oxidize nearby chlorophyll pigments and form highly delocalized charge-transfer states upon visible-light illumination. 1 mM DCBQ was found to divert 17.6% of the initial photoexcited electrons from their native path in wild-type *Synechocystis* cells, occurring within 600 fs. The addition of 3-(3,4-dichlorophenyl)-1,1-dimethylurea (DCMU), which binds to the QB pocket in PSII, to the reaction mix did not alter the kinetics. This confirmed that DCBQ acts in the early time frame within the photosynthetic pathway. This result was backed up with photoelectrochemical measurements which showed that DCBQ was capable of extracting electrons at an alternative site to Q_B and this contributed to around 30% of the photocurrent. PL spectroscopy also showed luminescence quenching correlating to DCBQ concentration, further emphasizing that DCBQ was interfering within the photosynthetic electron transport chain on the picosecond time scale. Oxygen evolution of PSII was unhindered by DCBQ suggesting the hole transport mechanism was not blocked. DCBQ concentrations greater than 200 μ M were found to be toxic to the cells after 12 h. The authors then genetically engineered the bacteria to lack either PSI or PSII. DCBQ addition to the PSI-less cells showed a lifetime decrease from 74 to 53 ps in the short lifetime component suggesting that DCBQ extracts electrons from PSII at longer timescales than the wild-type (<20 ps). In comparison, the PSII-less cells showed similar kinetics to the wild-type strains. Therefore, it was concluded that ET was primarily occurring from PSI to DCBQ. A similar result was also found with MV as an electron mediator. These results are crucial as they show that photoexcited reaction centers are not as insulated by protein scaffolds as previously thought. New research directions can now be investigated taking advantage of this ability to ‘rewire’ photosynthesis which will provide advances

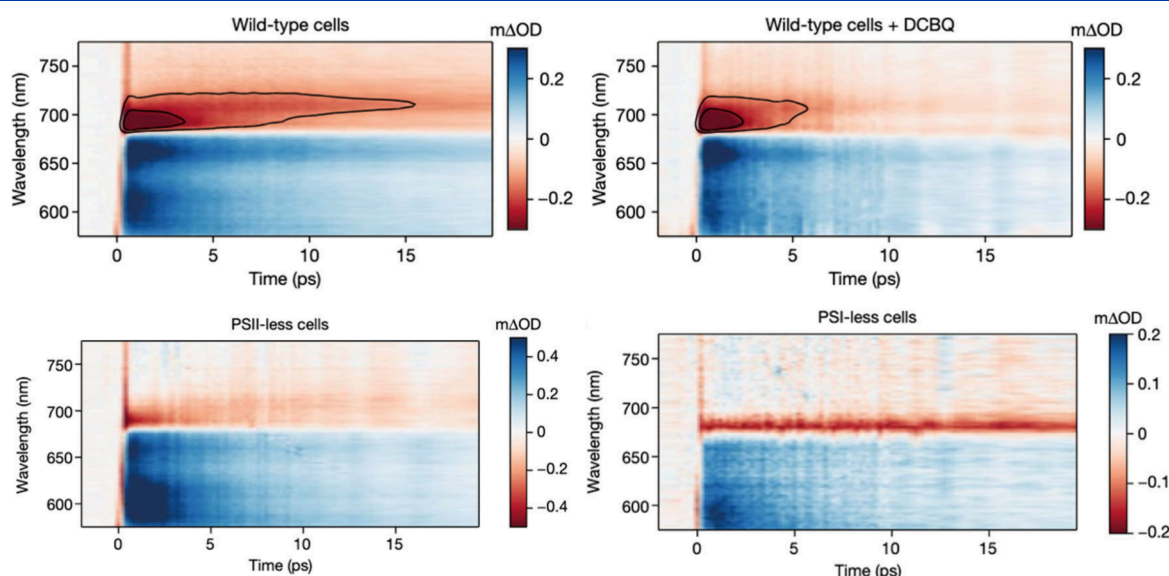


Figure 9. Ultrafast TA spectroscopy map of (Top) wild-type cells (left) and cells with DCBQ (right) (5 mM) between 2 and 20 ps photoexcited at 450 nm in units of differential absorption (m Δ OD). Two contours have been drawn at the same signal intensity to highlight the reduced lifetime of the 685 nm feature and suppression of the 715 nm rise on the addition of DCBQ. Maps are one sample, representative of several biological replicates (cells, $n = 8$, +DCBQ, $n = 5$).

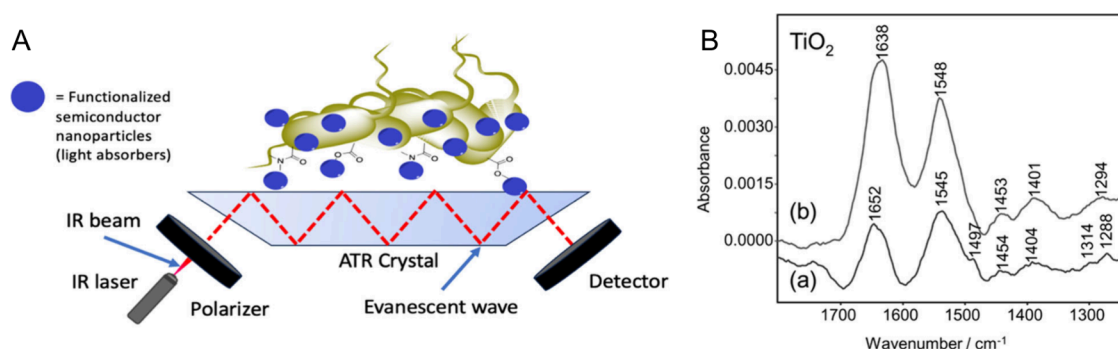


Figure 10. (A) Schematic of ATR-IR spectroscopy of biofilm of microbes coated with functionalized semiconductor nanoparticles (blue). (B) ATR-IR spectra of *P. aeruginosa* and TiO₂ nanoparticles. (a) Wild-type strain; (b) mutant strain that synthesizes reduced proteins (fpvA and fpvB) leading to less pyoverdine production. The spectra were collected after a 30-min period of bacteria (in water) being flowed across the prism. Reproduced with permission from ref 111. Copyright 2007 American Chemical Society.

in semiautomatic photosynthetic systems especially when using cyanobacteria for water oxidation. Performance of such devices can be evaluated based on their excited state lifetime which will give insights into charge separation and mitigation, reaction kinetics, and reducing energy losses. “Hacking” the electron transport chain opens the opportunity to develop a new range of mediator molecules which can improve STC efficiencies in SAP.

Time-Resolved Infrared Spectroscopy. Time-resolved infrared (TRIR) spectroscopy is used to investigate the molecular structure, the dynamics of molecular vibrations, and chemical reactions at the semiconductor biointerface on ultrafast timescales. Figure 7 shows a schematic of a typical pump–probe technique which can be used to study biohybrid systems. Structural changes, energy transfer processes, and reaction kinetics that occur during the conversion of light energy to chemical energy can be tracked. Changes in IR absorption or transmission are measured as a function of time.⁹³ In the context of microbial biohybrids for semiautomatic PS, TRIR can provide insights into the structural characteristics of biological systems, semiconductor materials, or catalysts upon excitation.⁹⁴ Once again, it is important to mention the challenges when working with living biological systems as there is limited transmission of IR radiation through water. Selectively probing with vibrations can allow one to track which functional groups are involved in the process. Additionally, vibrational modes can be monitored to gain insight into the kinetics of the processes. Practical examples of TRIR spectroscopy to semiconductor biohybrid systems are still scarce. On first look, this is surprising as there are many examples of TRIR with molecular CO₂ reduction catalysts. This is part of the reason why Re carbonyl complexes have been so popular.^{95–98} Molecular CO₂ catalysts have been developed side by side along with TRIR spectroscopy to study their structure and interactions.⁹⁹ Additionally, this is now the case with computational modeling where models are being used to assist in the discovery of new more efficient catalysts.^{100,101} Winkler, Gray, and co-workers studied the rate of electron transfer through metalloproteins.¹⁰² For example, using TRIR, they found that Re-Cu^(I/II) metalloproteins feature intermolecular electron transfer pathways. Spectroscopic analysis showed that the kinetics and electron transfer yields suggested that photoexcitation can lead to electron transfer within these protein dimers and that forward electron transfer is accelerated by interfacial tryptophan. Another example of TRIR applied to semibiological systems

is the work by Kelly and colleagues where they studied the photooxidation of natural DNA with enantiomerically pure Ru complexes.¹⁰³ TRIR spectroscopy allowed the authors to track the oxidation of guanine moieties within the DNA strands and provided information on the structure of the binding sites by recording TRIR before electron transfer occurred. These examples beg the question, why are these examples so scarce for microbial biohybrids? Perhaps challenges around the complexity of the system have hindered researchers from carrying out experiments or meaningfully interpreting very complicated data.

The commonly studied system of CdS- *M. thermoacetica* has been studied with TRIR and electron transfer was observed from the CdS NPs to membrane-bound proteins within the microbes.⁸⁷ TRIR spectra showed changes in amino residues as the amino groups are highly involved in the electron transfer pathways in H₂-incubated *M. thermoacetica*. This was discovered due to changes in C=O, C=N, and C≡N stretches 1760–1880 cm⁻¹ within the TRIR spectra. This provides key insight into the mechanism at the biointerface of *M. thermoacetica*. More work needs to be done with other microbes (e.g., *Geobacter sulfurreducens* and *S. ovata*) to develop a greater understanding of electron transfer at the biointerface of promising electrotrophic biohybrids.

Attenuated Total Reflectance Infrared Spectroscopy. Infrared (IR) spectroscopy (including spectroelectrochemistry (SEC)) has been used to study artificial catalysts for CO₂ reduction for decades. For example, molecular catalysts based on Re and Mn carbonyl complexes.¹⁰⁴ Hartl et al. used a combination of cyclic voltammetry (CV) and IR to study CO₂ coordination to Mo complexes. SEC results showed modest catalytic performance by the complexes toward formic acid production.¹⁰⁵ Another applicable example of utilizing IR spectroscopy is the work on metalloprotein chemistry. IR-SEC can be used to track direct electron transfer (DET) between electrodes and immobilized metalloproteins. Solution-phase IR spectroscopy represents specific challenges, as the IR absorption of the solvent can play a huge role, interfering with the vibrational modes of the dissolved or suspended material. Potentiostatic control is also difficult to be maintained in the specialized SEC cells which need to be as thin as possible to aid in minimizing solvent interference.¹⁰⁶ The broad IR absorbance of water makes it a challenge to identify other molecules present within samples. Furthermore, the highly polar nature of water presents issues as water molecules will interact with other strongly polar molecules

within samples, often distorting the spectra produced. Therefore, water is a far from ideal solvent for IR spectroscopic studies.

To overcome this, attenuated total reflectance (ATR) can be used in conjunction with infrared (IR) spectroscopy.^{107,108} ATR-IR uses a phenomenon known as total internal reflection which leads to the formation of an evanescent wave. The thickness of the water layer is minimized and multiple reflections or “bounces” are needed to enhance the signal quality. The wave extends to the sample, with the penetration depth depending on numerous factors including the wavelength of the incident photon and angle of incidence. By varying the angle and wavelength variations for the analysis of a biofilm sample (Figure 10).

Understanding the mechanism of microbial binding to semiconductors such as metal oxides is still a largely unanswered question in microbial SAP. Developing an understanding of the mechanisms of biofilm formation on an electrode will rapidly accelerate the ability to increase STC efficiencies and current densities. Parikh et al have previously used ATR-IR to demonstrate microbial attachment to hematite ($\alpha\text{-Fe}_2\text{O}_3$) and goethite ($\alpha\text{-FeOOH}$).¹⁰⁹ Biofilms of *Pseudomonas putida*, *P. aeruginosa*, and *E. coli* were grown on each mineral and the binding interactions were analyzed with ATR-IR. The results highlight the importance of phosphorus-containing groups and carboxyl groups in bacterial biofilm adhesion with adhesion of cells being overall similar to both metal oxides. This result leads to further questions like the binding of other microbes (e.g., electrotrophs) and how would the microbes interact with other non-Fe-containing minerals? The result highlights the potential of ATR-IR when studying the biointerface.

ATR-IR has also been used to elucidate the binding between *P. aeruginosa* biofilm and a ZnSe prism.¹¹⁰ It was found that the addition of Cr(III) nitrate to the solution resulted in binding between Cr(III) and bacterial exopolymers that were present on the surface of the ZnSe prism surface through electrostatic interactions. This resulted in moving the bacterial cell wall closer to the ZnSe prism. Further experiments were carried out on an engineered strain of *P. aeruginosa* which possessed extended surface exopolymers. The distance was found to be dependent on the presence of metal cations. Ni(II) and Co(II) ions were added to exchange with Cr(III) ions, it was found that Ni(II) and Co(II) displayed some affinity to the *P. aeruginosa* biofilm but not as much as Cr(III). IR spectroscopy did not appear to change noticeably upon the addition of metal cations indicating an electrostatic interaction between the cations and bacteria that occurs in the earliest stages of biofilm growth. This result can give researchers studying biohybrids an indication of which ions to incorporate within semiconductors that may increase binding affinities, biofilm formation and STC efficiencies. Once again, these experiments need to be reproduced with numerous microbes and numerous semiconductors to gain more concrete insight into the mechanisms.

In another example, the biofilm growth mechanism of *P. aeruginosa* to TiO_2 and Fe_2O_3 has been studied using in situ IR spectroscopy¹¹¹ (Figure 10B). It was subsequently found that the cells bind covalently to each metal oxide via a catechol ligand. This is a crucial observation for elucidating the mechanism of biofilm growth of bacteria that produce catechol-containing siderophores. The contrast between these two results, one showing electrostatic binding, and another

covalent binding highlights the uniqueness of each microbe and each semiconductor, each having different electronic properties.

However, examples of microbial biohybrids are limited and further work will be needed. Different microbes, for example, electrotrophic bacteria (e.g., *S. ovata*) are hypothesized to directly uptake electrons from electron donors such as photoexcited semiconductors but the mechanism of binding to materials like metal oxides is poorly understood at present.

Raman Spectroscopy. Raman spectroscopy can be used to study the vibrational and rotational modes of molecules within photoabsorbers and microbes, producing information on molecular structure and interactions between light and matter. Raman spectroscopy works by directing a laser beam at a sample and measuring the scattered light,¹¹² as illustrated in Figure 5E. Most light is scattered elastically, which is known as Rayleigh scattering. In this case, the wavelength of the incident and reflected photons remain constant. However, another form of scattering typically occurs, known as Raman scattering. Here, photons scattered have gained or lost energy based upon interacting with vibrating molecules within the sample. Raman scattering consists of both Stokes and anti-Stokes scattering. Stokes scattering occurs when scattered photons have lower energy than incident photons, hence energy has been lost within molecular vibrations. The reverse is true for anti-Stokes scattering; the reflected photons have gained energy from molecular vibrations. Vibrational modes can correspond to energy peaks within the Raman spectrum, providing a fingerprint of molecular vibrations that are unique to each chemical structure.

In terms of the application of Raman spectroscopy in the field of microbial biohybrids for semiartificial PS, Raman can be used to analyze biomolecules such as proteins within the microbes, but the important advantage is that, unlike TRIR and ATR-IR, water is no longer an issue. The key difference between Raman and IR is that in Raman, scattered light with changes in frequency corresponds to vibrational quanta whereas in IR spectra vibrational excitation must result in a change in dipole moment with the analyte for the radiation to be absorbed. Raman can also be used for probing redox reactions by monitoring Raman shifts of redox-active molecules. Intermediates can be detected, and structural changes can be assessed.

Chen et al. have reported *Halobacterium* purple membrane-derived vesicles which were integrated with TiO_2 NPs doped with Pd within the pores.¹¹³ The biohybrid used *bacteriorhodopsin* as a natural dye to sensitize the TiO_2 and inject photoexcited electrons into the conduction band of the TiO_2 . This biohybrid could reduce CO_2 into CO and CH_4 . CH_4 production was much more impressive than the CO production and became very noticeable after 2 h. After 8 h, 451.3 mmol $\text{g}_{\text{catalyst}}^{-1}$ of CH_4 was produced with a 95.2% selectivity. The biological function of the *bacteriorhodopsin* is maintained within the system allowing proton pumping to occur within the biohybrid. In this example, Raman spectroscopy was used to prove the successful integration of the NPs and the *bacteriorhodopsin*. Femtosecond TAS was also utilized here to probe the electron transfer from *bacteriorhodopsin* to TiO_2 .¹¹³ TAS experiments were able to calculate lifetimes for each of the samples, PM had a lifetime of 1.08 ± 0.05 ps, *Halobacterium* purple membrane-derived vesicles had a lifetime of 1.05 ± 0.09 , and when fused with palladium-deposited porous hollow TiO_2 nanoparticles the lifetime was quenched

to 270 fs \pm 0.01, indicating charge transfer from the excited bacteriorhodopsin to TiO₂ NPs with an efficiency of 74.3%. By utilizing a combination of spectroscopic techniques researchers were able to propose this electron transfer mechanism within the biohybrid.

In 2020, Ye et al. integrated CdS QDs decorated with Ni NPs with *Methanosarcina barkeri* to convert CO₂ into methane.¹¹⁴ The effect of Ni doping (0.75%) was found to enhance CO₂ to methane conversion by over 250% when compared to the Ni-free sample. In these systems, it was observed that Ni acts as an electron sink which can accelerate electron transfer under illumination. Moreover, Ni can alter the metabolic pathways within *M. barkeri*. Expression of proteins known to aid in electron transfer e.g. inorganic ion transport proteins was found to be upregulated in samples doped with Ni. Here, Raman spectroscopy was shown to demonstrate the successful integration of CdS QDs in samples with and without Ni with a peak at 300 cm⁻¹ which was attributed to the distinct signal of a Cd-S bond, confirming the successful attachment of the QDs to the microbes.

A final example of Raman being used in semiconductor biohybrid systems is the nanoencapsulated CdS- *E. coli* within tannic acid – Fe complexes to increase the stability of bacteria within seawater and improve photocatalytic H₂ evolution. Raman spectroscopy aided in probing the integration of the tannic acid – Fe complexes around bacteria. Peaks at 1348 cm⁻¹ and 1485 cm⁻¹ were observed which were attributed to the stretching of C-C bonds within phenyl rings and C-H bond bending within the tannic acid, respectively.¹¹⁵ The Raman spectra confirmed the successful coating of a protective coating composed of tannic acid–Fe complexes. The *E. coli*@Tannic acid@CdS produced a photocurrent density of 1.6 mA cm⁻², while the *E. coli*@tannic acid sample produced only 800 nA cm⁻² and the sole *E. coli* sample produced 400 nA cm⁻². This is a good example of how Raman spectroscopy can be used to understand and develop new and improved microbial biohybrids.

X-ray Spectroscopy. X-ray absorption spectroscopy (XAS) probes the electronic and structural properties of materials by measuring the absorption of high-energy photons (X-rays), as shown in Figure 5D.¹¹⁶ Information can be gathered relating to the environment of the microbe on the semiconductor surface in a BPEC system or in a photocatalytic system. It can also provide insights into the electronic structure of the photoactive material. Catalyst activation and deactivation can also be tracked. Reaction mechanisms can be interpreted by studying XAS spectra under varying reaction conditions. However, the obvious challenge is exposing living biohybrid samples to high-energy X-rays will very quickly lead to sample degradation. In-situ and operando XAS can also give insights into how well a system is performing to maximize solar fuel production and what the bottlenecks may be. For example, Lewerenz et al. used XAS and computations to study the efficiency of artificial solar fuel light absorbers and catalysts.¹¹⁷ XAS allowed the authors to conclude that Fe doping improved the efficiency of a NiOOH electrocatalyst. In XAS, a sample is exposed to a beam of monochromatic or polychromatic X-rays and an absorbance spectrum is taken. The resulting spectrum is affected by inelastic scattering and photoelectric absorption. Photoelectric absorption involves the ejection of an electron from a lower energy level than the valence electrons leaving what is known as a core hole. This absorption has a specific energy depending upon the element and environmental

conditions it is found. XAS can be useful when analyzing microbial biohybrids to probe light-absorbing materials and catalysts, investigating their electronic properties before and after the incorporation of microbes. Redox processes can be tracked within the biohybrid by monitoring oxidation states within the system, e.g., in metalloproteins. Lastly, electron transfer dynamics can be tracked using XAS by analyzing the electronic structures of the components within the biohybrids in tandem with other spectroscopic techniques, e.g., TAS or electrochemistry.

X-ray photoelectron spectroscopy (XPS) is a surface-sensitive technique that can analyze the elemental composition of materials. In XPS, a sample is bombarded with X-rays, usually monochromatic. In a similar way to XAS electrons are ejected from core energy levels from atoms at the surface of the material. These ejected electrons are known as photoelectrons which hold information within them that corresponds to the elemental structure and environment of a material, as shown in Figure 5C. The kinetics of the photoelectrons detected can be interpreted in terms of chemical state, bonding, electronic structure, and elemental composition.¹¹⁸ Li et al. utilized operando XPS to study IrO_x catalysts in a water oxidation system.¹¹⁹ In this example, XPS studying the catalysts under OER conditions Ir was found to change oxidation state from +4 to +5, mostly on the surface of the catalyst. This chemical alteration was found to correlate to a decrease in surface hydroxide. The authors therefore hypothesized that OER on the IrO_x surface occurs through an OOH-mediated protonation.

In terms of application to microbial biohybrids, XPS can be used to characterize the surface chemistry, study the biointerface, monitor redox chemistry, track surface modifications upon the addition of microbes, and study the stability of the biohybrids. X-ray spectroscopy can also be utilized to monitor factors such as oxidation states of metal centers in proteins. The process of electron transfer between semiconductor to microbe alters the oxidation state (e.g., within cytochromes). However, there are still challenges to consider in such systems, including the penetration depth, sample stability to X-ray bombardment, and adding techniques simultaneously to provide time resolution to the measurements.

Materials, both natural and synthetic, meet microbes in many scenarios, for example within water pipes, oil platforms or bioreactors. Despite this, spectroscopic studies of these interactions and how these interactions can affect the cell surface of the microbes are scarce perhaps due to the complexity of sample preparation and difficulties interpreting generated spectra. X-ray spectroscopy in particular presents difficulties as one must be careful not to destroy the samples by bombarding them with high-energy X-rays. XPS can be used to measure properties such as surface charge and hydrophobicity on the surface of microbes. These properties can then be used to understand the physical properties of microbial interactions.¹²⁰ XPS has been utilized in the characterization of the electronic structure of CdS QDs which were then combined with different microbes for photosynthesis of useful chemicals. Wang et al. used XPS to confirm the attachment of CdS QDs to the surface of *Rhodospseudomonas palustris* for the photocatalytic production of carotenoids and poly- β -hydroxybutyrate (PHB) from waste CO₂.⁴⁸ Similarly, the attachment of CdS QDs to *M. barkeri* for the conversion of CO₂ to methane.⁴⁴ In both cases, XPS confirmed the presence of Cd²⁺

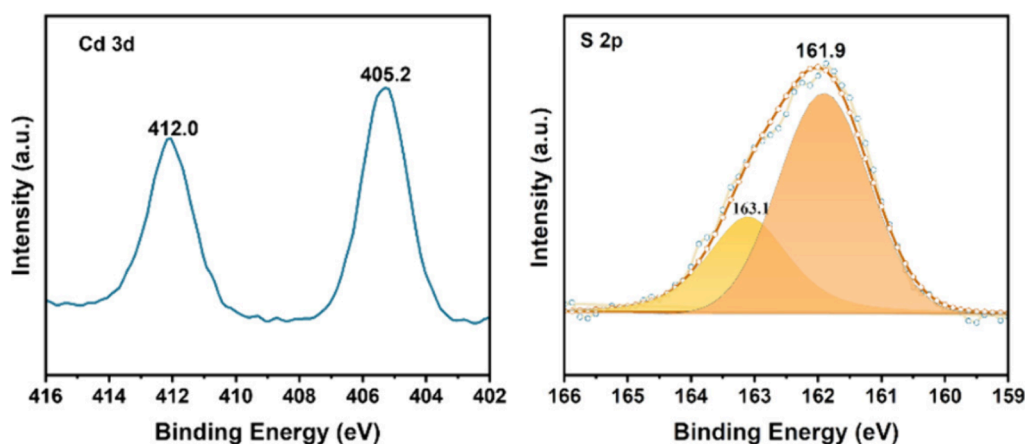


Figure 11. XPS spectra of the CdS nanoparticles attached to the surface of *S. oneidensis*: Cd 3d and S 2p. Reproduced with permission from ref 121. Copyright 2023 Royal Society of Chemistry Publishing.

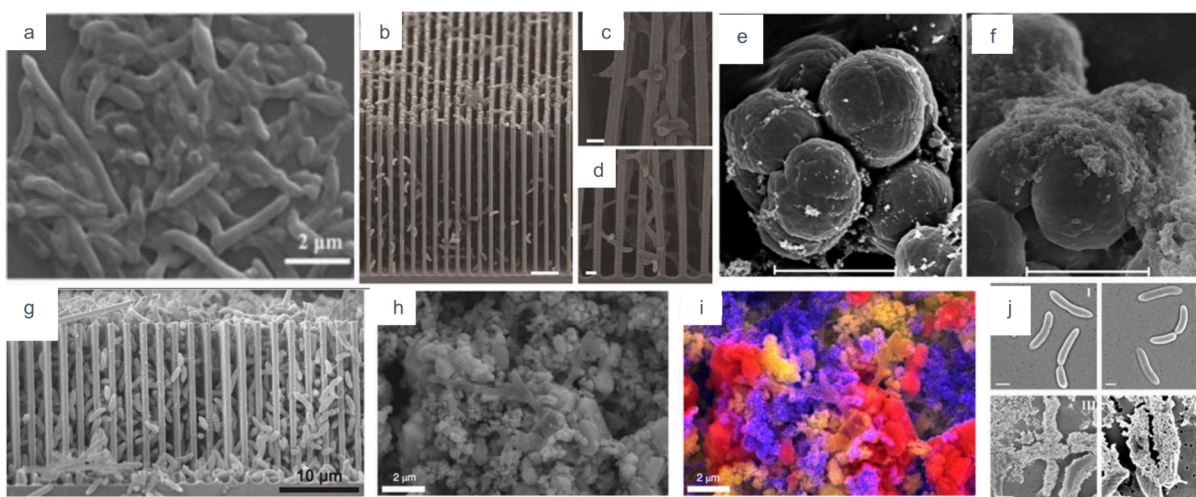


Figure 12. SEM images of a variety of semiconductor microbial biohybrids. (a) Conjugated polymers (CPN-TA) on the surface of *R. palustris*. (b–d) *S. ovata* integrated onto SiNWs. (e, f) CdS on the surface of *M. barkeri*. (g) Close-packed *S. ovata* on SiNWs, showing increased quantities of *S. ovata* at the biointerface. (h, i) *S. ovata*/Cr₂O₃/Ru-SrTiO₃:La,Rh/ITO/RuO₂-BiVO₄:Mo sheet after a 15 h photosynthetic reaction. (j) CdS NPs on the surface of *S. ovata*. Reproduced with permission from ref 44. Copyright 2019 Elsevier Publishing; ref 64. Copyright 2020 Elsevier Science and Technology Journals; ref 62. Copyright 2015 American Chemical Society; ref 56. Copyright 2022 Springer Nature BV; ref 124. Copyright 2022 American Chemical Society; ref 125. Copyright 2020 American Chemical Society.

and S²⁻ on the cell membrane of the microbes confirming successful photosensitization of the cells.

Furthermore, Liu et al. used XPS to verify the successful attachment of the CdS to *S. MR-1* where CO₂ reduction efficiencies were improved using an electron conduit within the electroactive bacterium¹²¹ (Figure 11). This activity has been linked to two hydrogenase enzymes within the periplasmic space of *S. oneidensis*.¹²² As a result of this, charge recombination was inhibited and formate production from CO₂ was enhanced with a maximum rate of formate production being 2650 μmol g⁻¹ h⁻¹ with a near 100% selectivity. The reported photocurrent densities were 1.06 mA cm⁻² for CdS and 3.8 mA cm⁻² for CdS@*S. oneidensis*. This value represents one of the most efficient colloidal semiconductor–biohybrid systems reported to date.

Electron Microscopy. Electron microscopy can be used to study the structure and morphology of materials at the biointerface with very high magnification and resolution. When applied to semiconductor biointerfaces of living microbial photohybrids, electron microscopy can provide valuable

insights into the interactions between semiconductors and microorganisms. The two main forms of electron microscopy are transmission and scanning electron microscopy (TEM and SEM). SEM is a surface analysis technique which involves scanning a sample with an electron beam which results in the emission of secondary electrons which can be detected and interpreted to form an image. For semiconductor biohybrids, SEM can be particularly useful for observing microbial binding within the pores and on the surface of semiconductors under different environmental conditions. TEM is a similar technique however in this case an electron beam is transmitted through a thin sample, producing high-resolution images of the internal structure. Interactions between bacteria and semiconductor NPs can be imaged, which is extremely beneficial when interpreting what is happening at the interface. TEM can also give details of cell structure and how organelles are arranged within microbial cells.¹²³ The main challenge with electron microscopy is that the sample must be dead and be fixed before it can be measured which makes it not possible to view biofilm formation in situ.

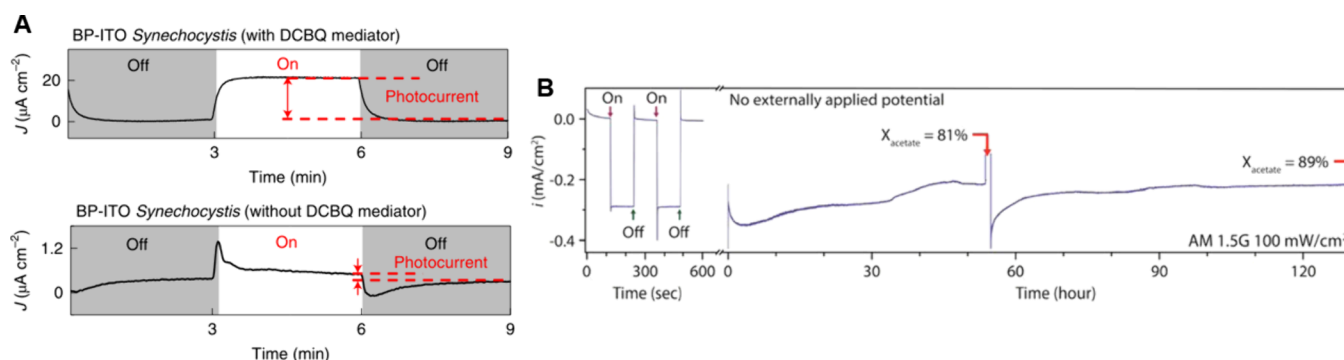


Figure 13. (A) Representative photocurrent profile obtained from a *Synechocystis*-loaded BP-ITO electrode in the presence and absence of the exogenous electron shuttle DCBQ (1 mM). (B) Unassisted solar-powered acetate production from the SiNW- *S. ovata* hybrid device. Chronoamperometry under illumination for 6 days. During the experiment the atmosphere was 20% CO_2 /80% N_2 . X_{acetate} represents the faradaic efficiency of acetate at the end of the experiment. Reproduced with permission from refs 55 and 64. Copyright 2022 Springer Nature BV; Copyright 2020 Elsevier Science and Technology Journals.

Figure 12 shows a collection of SEM images showing the importance of using electron microscopy to visualize semi-artificial photosynthetic biohybrids. Another example of the advantages of using electron microscopy to study the biointerfaces of these systems was shown by Yang et al.⁶² where unassisted solar acetate production was reported using a biohybrid photocathode composed of Si NWs as the light absorber and *S. ovata* as the biological cocatalyst (Figure 12b–d). Here, cross-sectional SEM was carried out to image the three-dimensional biointerface along with magnified images at varying depths being reported. SEM images revealed that the bacteria incorporated themselves within the 3D network of Si NWs, increasing the surface area of the biointerface, and leading to enhanced STF efficiencies.

In 2020, Yang followed up with a report of a close-packed nanowire-*S. ovata* biohybrid with an increased CO_2 -to-acetate conversion efficiency (3.6% over 1 week)⁶⁴ (Figure 12g). By controlling the local pH at the biointerface the surface coverage of the NWs by the bacteria can be vastly improved. A pH of 9.3 within the nanostructures of the cathode was found to be an incompatible environment for *S. ovata*. Further investigations into pH found that controlling the pH around the electrode to 6.4 produced a highly close-packed optimum structure. Optimizing the pH vastly improved performance from $\sim 0.3 \text{ mA cm}^{-2}$ for the unoptimized system to $> 0.45 \text{ mA cm}^{-2}$. Once again, cross-sectional SEM was used to visualize these findings. The resulting electrode produced a CO_2 -reducing current density of up to approximately 0.65 mA cm^{-2} . The electrochemical setup was then coupled to an external PV device which enabled highly efficient solar-to-acetate production with an efficiency of 3.6% over 7 days. However, it is important to note that within this system simply applying a more negative potential did not increase the acetate production. Faradaic efficiencies at a variety of potentials suggested that more negative potentials ($\leftarrow 1.1 \text{ V}$ vs SHE) favored H_2 evolution over acetate production.

The unassisted bacteria biohybrid photosheet reported by Reisner et al. (previously discussed above) was also studied using electron microscopy⁵⁶ (Figure 12g,h). SEM was carried out on the *S. ovata*/Cr₂O₃/Ru-SrTiO₃:La, Rh/ITO/RuO₂-BiVO₄:Mo sheet after illuminating for 15 h. SEM energy dispersive spectroscopy (SEM-EDS) was also carried out which allowed for the mapping of individual elements present

throughout the biointerface to map the different elements present that *S. ovata* had attached to.

Colloidal photocatalytic systems which produced methane from CO_2 have also been examined using electron microscopy. CdS-*M. barkeri* was studied by both SEM and TEM showing the attachment of the CdS semiconductors to the surface of the microbes (Figure 12e,f). SEM-EDS was also reported showing both the elemental mapping for Cd and S.⁴⁴ In a similar colloidal system containing CdS and *S. ovata* for acetate production (Figure 12j), SEM was utilized to observe the attachment of the NPs to the surface of the microbes.¹²⁴ Organic conjugated polymers can also be visualized on the surface of microbes. For example, on the surface of *R. palustris* the integrated conjugated polymers onto the surface of *R. palustris* for enhanced photocatalytic H_2 evolution (shown in Figure 12a).¹²⁵ These examples highlight the importance of electron microscopy in imaging the biointerface. SEM and TEM are key to optimizing biohybrid systems on the nano- and micro-scale.

Advanced Electrochemical Methods. The use of advanced electrochemistry to study and optimize redox reactions occurring within biohybrids, especially systems that consist of microbes immobilized on an electrode surface is a crucial analytical technique for calculating system efficiencies. Techniques such as impedance spectroscopy, cyclic voltammetry, chronoamperometry, and linear sweep voltammetry can be used to understand the redox behaviors of species within biohybrids.^{126,127} Redox-active molecules within the microbes such as metalloproteins can be studied by measuring factors such as redox potentials, current–voltage responses, and even charge transfer kinetics. Spectroelectrochemistry which combines an electrochemical measurement with a spectroscopic technique is also very powerful. For example, by recording changes in absorbance using UV–visible spectroscopy whilst varying the applied voltage to follow changes in an oxidation state. Spectroscopic techniques can detect changes in the electronic or vibrational properties within the microbial biohybrids under different electrochemical environments. Challenges include technical issues in sample and cell preparation and sample complexity. Variation between samples can also provide difficulties. However, the quality of information gained once the technical challenges have been overcome far outweighs the challenges.

Chen et al. utilized electrochemistry to study the performance of 3D-printed electrodes composed of ITO NPs and a cyanobacterium *Synechocystis* sp. PCC 6803. With 600 μm micropillars, a mediated photocurrent of 245 $\mu\text{A cm}^{-2}$ was produced which is the closest so far to the theoretical maximum for this kind of system. An external quantum efficiency of up to 29% was also reported using monochromatic red (680 nm) light at 1 mW cm^{-2} . In this work, amperometry and cyclic voltammetry (CV) were employed extensively to study the electrochemistry of the system. CV was used to measure the capacitance of the systems by varying the scan rate. Chronoamperometry was carried out with and without mediators at 0.3 and 0.5 V vs SHE. A steady-state photocurrent of 20 $\mu\text{A cm}^{-2}$ was shown upon the addition of a redox mediator⁵⁵ (Figure 13A). Electrochemical responses can be used to track the effects of the addition of a mediator.

Electrochemical analysis of enzyme biohybrids can be used to aid in fundamental understanding in microbial systems. For example, PSII biofilms coated on ITO electrodes.¹²⁸ In vivo, PSII is repaired every 15 min due to its sensitivity to incoming light. When PSII has been loaded onto artificial electrodes for example ITO similar lifetimes are observed.¹²⁸ Wiring whole-cell cyanobacteria on inverse-opal ITO electrodes with pores of around 10 nm have been reported to produce stable photocurrents of 700 nA cm^{-2} and biofilms were found to be stable on the ITO electrodes for more than 5 days using UV-vis absorption spectroscopy.⁵⁸ Over time, the performance was enhanced which was attributed to improved wiring of cyanobacteria to the surface of the ITO. Photocurrent densities of the whole-cell cyanobacteria (700 nA cm^{-2}) were still much lower than individual enzyme-based systems (<15 mA cm^{-2}) despite the enhanced stability. CV was carried out in the dark and under illumination to observe any light-induced redox processes. It was found that light induced a redox wave which was possibly produced from the redox mediators added to the system.¹²⁹

Time-resolved spectroelectrochemistry of biohybrid photoelectrodes has been reported by Nawrocki et al.¹³⁰ The redox states of the reaction center light-harvesting complex (RC-LH1) of *Rhodospirillum rubrum* absorbed on the surface of mesoporous ITO. Time-resolved spectroelectrochemical measurements were carried out to allow kinetic bottlenecks within the electrode to be identified. Photocurrent responses were recorded and oxidation states within RC's were tracked. Analysis showed kinetic bottlenecks within the biohybrid and processes which result in energy losses throughout the electron transfer steps. It was found that 73% of energy loss arose from short-circuiting of charge-separated states at the semiconductor/biointerface with 60% of RC's remaining inactive in electron transfer to the ITO electrode due to bottlenecks at the interface. This study demonstrates a key example of how electrochemistry can be paired with spectroscopy to unravel the immense potential of performing catalysis with biohybrid devices. Figure 13B demonstrates the stability of a TiO_2 NW/Si NW/*S. ovata* biohybrid, which was found to have a Faradaic efficiency of 89%, with a photocurrent density = -0.2 mA cm^{-2} after 120 h of operation.⁶²

Microbiological Methods. Microbiologists also have a crucial role to play in elucidating the mechanisms occurring at the semiconductor-microbe biointerface.^{79,131,132} The use of molecular biology techniques such as transcriptional analysis and proteomics can provide key insights into gene expression and protein profiles of the microorganisms involved. The

difficulty with these techniques is that for a large proportion of the relevant microbes, a genetic toolkit has not yet been identified. For example, the work by Lovley and co-workers on studying and engineering electrotrophic microbes has been revolutionary. *Geobacter sulfurreducens* has been demonstrated to use electrodes as an electron donor and can convert fumarate to succinate¹³³ or as an electron acceptor converting acetate to CO_2 and producing electricity by donating electrons to an electrode (microbial fuel cells).^{134,135} *G. sulfurreducens* have been found to produce up to 3 mA cm^{-2} on IO-ITO electrodes at a poised potential of 0.1 vs SHE, highlighting the conductive nature of *G. sulfurreducens*.¹³³ *G. sulfurreducens* produces conductive protein pili nanowires which aid in electroactivity.¹³⁶ Lovley et al. were able to isolate a more conductive strain of *G. sulfurreducens* (KN400) by incubating *G. sulfurreducens* at $-400 \text{ mV vs Ag/AgCl}$ for 5 months and then isolating the sample from the electrode surface and reculturing.¹³⁷ KN400 produces more conductive nanowires and biofilms were found to have a conductivity of over 300 mS cm^{-1} which correlated to a high nanowire abundance.¹³⁸

Another example is a study by Ueki et al. where metabolic engineering was used to redirect the metabolism of *Clostridium ljungdahlii* to produce butyrate over acetate directly from CO_2 .¹³⁹ Results demonstrated that it was possible to redirect toward butyrate through genetic mutations redirecting carbon and electron pathways. The authors conclude by adding that it is important to take this work to the next step by improving selectivity and making butyrate the sole product from the metabolism by redirecting the natural carbon flux.

By studying the expression of different genes within the microbe through transcriptional analysis, using techniques such as microarrays or RNA sequencing, genes directly involved in the uptake of electrons from the semiconductor can be identified. Genes directly involved in the process will be observed to be up-regulated during photo experiments. For example, the work discussed earlier where protein expression was studied and an upregulation of inorganic ion transport proteins was found in photohybrids with *M. barkeri*, Ni and CdS.¹¹⁴ Furthermore, Zhang et al. studied protein and metabolite expression in a *M. thermoacetica*-CdS biohybrid under light illumination.¹⁴⁰ It was found that during the light-harvesting process, the Wood-Ljungdahl pathway was activated by the presence of CdS. Upon quantification of metabolites, results showed activation of energy-metabolism-associated glycolysis and the tricarboxylic acid (TCA) cycle. The authors proposed an energy-conversion mechanism within the biohybrid. This means glycolysis and TCA occurred as well as acetyl coenzyme A and NADH oxidation.

This information can then be used to aid microbiologists when genetically engineering these microbes to perform more efficiently within the photobiohybrids. Proteomic analysis is another key tool within the microbiology toolkit that can be used to study protein expression within microbes. Mass spectrometry-based proteomics is particularly useful in identifying and quantifying proteins present under different conditions and within different microbes. Protein-protein interactions can be tracked and their involvement at the biointerface can be calculated. Regulatory proteins and key enzymes can be identified, allowing for the metabolic and signaling pathways to be elucidated with the microbial section of the system. Proteomics can also be integrated with transcriptional data to analyze metabolic pathways by mapping gene expression with protein expression.

FUTURE PERSPECTIVES

The field of semiartificial photosynthesis, where living microbes meet state-of-the-art photoactive materials, offers vast opportunities. Using the lens of spectroscopy, the secrets of intracellular and extracellular electron transfer can be unravelled by measuring the ultrafast process of electrons passing through the cell membranes of living electrotrophic organisms. The research community must now focus on the major bottlenecks within the field. Here, we have discussed a wide range of techniques, but through multidisciplinary collaboration, the field can be accelerated to address pressing challenges such as the urgency and scale of net zero. Faradaic efficiencies of the biohybrids must be amplified along with controlling product selectivity. STC conversion efficiencies must be pushed to huge heights, surpassing 10%, which is of crucial importance for commercial scalability. Reaching this pivotal threshold will allow for the “solar fuels/chemicals” to be used as chemical feedstocks for endless industrial applications and replace the current feedstocks which originate from hydrocarbons derived from fossil fuels. Major advancement is needed within both the biotic and abiotic components of the biohybrids. An earth-abundant, scalable oxygen-evolution catalyst must be developed beyond current technologies,¹⁴¹ as water oxidation is inherently “sluggish” and high applied potentials are needed for efficient water oxidation. Critically, PV components of the biohybrids require rigorous optimization by trialling new earth-abundant materials with ideal bandgaps and improving current materials, e.g. via doping, to improve solar light absorption and quantum efficiency. These materials will need to be fine-tuned and optimized for the conversion of solar photons into chemical bonds, especially energy-rich C–C bonds. Optimizing these factors will unlock the full potential of the PV.

Delving into the photophysics of the semiconductor biointerfaces using contemporary spectroscopy can unveil the biggest bottlenecks within the systems. Theoretical data using bioinformatics and density functional theory (DFT) can also aid in unravelling the mysteries of the system and forge a path through the obstacles that currently hinder progress within the field. Using the eyes of electron microscopy, a vivid picture of the biointerface can be painted, displaying the synergy between semiconductors and bacteria and how different morphological configurations hinder or improve STC efficiencies. Electrochemistry can orchestrate biohybrid optimization via tracking redox reactions. A final instrument in the armory is the synthetic biology toolkit, unleashing the potential to engineer the microbes to increase their electron uptake and chemical output. In conclusion, a series of monumental innovations are necessary for industrially useful sustainable chemical production. Microbial biohybrids are a relatively recent development but are already at the forefront of sustainable energy technology research, paving the way to a greener future globally.

AUTHOR INFORMATION

Corresponding Authors

Elizabeth A Gibson – *Energy Materials Laboratory, Chemistry, School of Natural and Environmental Science, Newcastle University, Newcastle upon Tyne NE1 7RU, United Kingdom*; orcid.org/0000-0002-6032-343X; Email: elizabeth.gibson@newcastle.ac.uk

Shafeer Kalathil – *Hub for Biotechnology in the Built Environment, Faculty of Health and Life Sciences, Department of Applied Sciences, Northumbria University, Newcastle NE1 8ST, United Kingdom*; Email: shafeer.kalathil@northumbria.ac.uk

Authors

Cathal Burns – *Hub for Biotechnology in the Built Environment, Faculty of Health and Life Sciences, Department of Applied Sciences, Northumbria University, Newcastle NE1 8ST, United Kingdom; Energy Materials Laboratory, Chemistry, School of Natural and Environmental Science, Newcastle University, Newcastle upon Tyne NE1 7RU, United Kingdom*

Linsey Fuller – *Procter and Gamble Company, Procter and Gamble Innovation Centre, Newcastle upon Tyne NE12 9TS, United Kingdom*

Complete contact information is available at: <https://pubs.acs.org/10.1021/aps.4c00008>

Author Contributions

C.B. wrote and reviewed the manuscript. E.A.G. and S.K. provided feedback on the manuscript and aided in the writing and reviewing process. E.A.G., L.F., and S.K. acquired the funding and supervised the project.

Notes

The authors declare no competing financial interest.

ACKNOWLEDGMENTS

This work was supported by BBSRC and was written in a partnership between Northumbria University, Procter and Gamble, and Newcastle University as part of the Biosciences for Sustainable Consumer Products Collaborative Training Programme (BISCOP CTP).

DEFINITIONS

Photoelectrochemistry- the study of chemical reactions that occur at the photoactive electrode–electrolyte interface under dark and illumination conditions. The principles of photochemistry and electrochemistry are employed to investigate solar energy conversion and processes such as water splitting.

Solar Chemicals- chemical reactions that are driven by solar energy are known to produce solar chemicals, typically via processes like photocatalysis or photoelectrochemistry. These chemicals can contribute to renewable energy and sustainable solutions by producing fuels and industrial feedstocks.

Microbial Photocatalysis- a process where microorganisms are combined with a semiconductor to harness light to power chemical reactions. The process takes advantage of the natural metabolic pathways of microbes combined with photoactive materials to efficiently convert solar energy and abundant resources (CO₂, N₂, H₂O) into chemicals or fuels.

Biointerface- a region where a biological entity, e.g., a microorganism, interacts with a synthetic material e.g. an inorganic semiconductor. This interface is critical in optimizing the efficiency of semiartificial photosynthetic systems.

Electrocatalyst- a material at an electrode surface that facilitates and accelerates electrochemical reactions, reducing the activation energy required for the reaction to occur.

Electrocatalysts are very important in energy conversion and storage technologies.

REFERENCES

- (1) Vera, I.; Langlois, L. Energy indicators for sustainable development. *Energy* **2007**, *32* (6), 875–882.
- (2) Erb, K.-H.; Gingrich, S. Biomass—Critical limits to a vital resource. *One Earth* **2022**, *5* (1), 7–9.
- (3) Barber, J.; Tran, P. D. From natural to artificial photosynthesis. *Journal of The Royal Society Interface* **2013**, *10* (81), No. 20120984.
- (4) McConnell, I.; Li, G.; Brudvig, G. W. Energy conversion in natural and artificial photosynthesis. *Chem Biol* **2010**, *17* (5), 434–447.
- (5) Whang, D. R.; Apaydin, D. H. Artificial Photosynthesis: Learning from Nature. *ChemPhotoChem* **2018**, *2* (3), 148–160.
- (6) Wang, X.; Sun, Q.; Gao, J.; Wang, J.; Xu, C.; Ma, X.; Zhang, F. Recent Progress of Organic Photovoltaics with Efficiency over 17%. *Energies* **2021**, *14* (14), 4200.
- (7) Muñoz-García, A. B.; Benesperi, I.; Boschloo, G.; Concepcion, J. J.; Delcamp, J. H.; Gibson, E. A.; Meyer, G. J.; Pavone, M.; Pettersson, H.; Hagfeldt, A.; et al. Dye-sensitized solar cells strike back. *Chemical Society Reviews* **2021**, *50* (22), 12450–12550.
- (8) Assadi, M. K.; Bakhoda, S.; Saidur, R.; Hanaei, H. Recent progress in perovskite solar cells. *Renewable and Sustainable Energy Reviews* **2018**, *81*, 2812–2822.
- (9) Sun, Z.; Chen, X.; He, Y.; Li, J.; Wang, J.; Yan, H.; Zhang, Y. Toward Efficiency Limits of Crystalline Silicon Solar Cells: Recent Progress in High-Efficiency Silicon Heterojunction Solar Cells. *Advanced Energy Materials* **2022**, *12* (23), No. 2200015.
- (10) Su, J.; Vayssieres, L. A Place in the Sun for Artificial Photosynthesis? *ACS Energy Letters* **2016**, *1* (1), 121–135.
- (11) El-Khouly, M. E.; El-Mohsawy, E.; Fukuzumi, S. Solar energy conversion: From natural to artificial photosynthesis. *Journal of Photochemistry and Photobiology C: Photochemistry Reviews* **2017**, *31*, 36–83.
- (12) Yang, W.; Prabhakar, R. R.; Tan, J.; Tilley, S. D.; Moon, J. Strategies for enhancing the photocurrent, photovoltage, and stability of photoelectrodes for photoelectrochemical water splitting. *Chemical Society Reviews* **2019**, *48* (19), 4979–5015.
- (13) Ismail, A. A.; Bahnemann, D. W. Photochemical splitting of water for hydrogen production by photocatalysis: A review. *Solar Energy Materials and Solar Cells* **2014**, *128*, 85–101.
- (14) Queyriaux, N.; Kaeffer, N.; Morozan, A.; Chavarot-Kerlidou, M.; Artero, V. Molecular cathode and photocathode materials for hydrogen evolution in photoelectrochemical devices. *Journal of Photochemistry and Photobiology C: Photochemistry Reviews* **2015**, *25*, 90–105.
- (15) Zhang, J.; Cui, J.; Eslava, S. Oxygen Evolution Catalysts at Transition Metal Oxide Photoanodes: Their Differing Roles for Solar Water Splitting. *Advanced Energy Materials* **2021**, *11* (13), No. 2003111.
- (16) Li, C.; He, J.; Xiao, Y.; Li, Y.; Delaunay, J.-J. Earth-abundant Cu-based metal oxide photocathodes for photoelectrochemical water splitting. *Energy & Environmental Science* **2020**, *13* (10), 3269–3306.
- (17) Yang, W.; Moon, J. Recent Advances in Earth-Abundant Photocathodes for Photoelectrochemical Water Splitting. *ChemSusChem* **2019**, *12* (9), 1889–1899.
- (18) Yang, Y.; Niu, S.; Han, D.; Liu, T.; Wang, G.; Li, Y. Progress in Developing Metal Oxide Nanomaterials for Photoelectrochemical Water Splitting. *Advanced Energy Materials* **2017**, *7* (19), No. 1700555.
- (19) Hisatomi, T.; Kubota, J.; Domen, K. Recent advances in semiconductors for photocatalytic and photoelectrochemical water splitting. *Chem. Soc. Rev.* **2014**, *43* (22), 7520–7535.
- (20) Reece, S. Y.; Nocera, D. G. Proton-Coupled Electron Transfer in Biology: Results from Synergistic Studies in Natural and Model Systems. *Annu. Rev. Biochem.* **2009**, *78* (1), 673–699.
- (21) Halmann, M.; Ulman, M.; Aurian-Blajeni, B. *Sol. Energy* **1983**, *31* (4), 429.
- (22) Ogura, K.; Yoshida, I. Electrocatalytic reduction of carbon dioxide to methanol—VI. Use of a solar cell and comparison with that of carbon monoxide. *Electrochimica acta* **1987**, *32* (8), 1191.
- (23) Alberio, J.; Peng, Y.; García, H. Photocatalytic CO₂ Reduction to C₂+ Products. *ACS Catalysis* **2020**, *10* (10), 5734–5749.
- (24) Kornienko, N.; Zhang, J. Z.; Sakimoto, K. K.; Yang, P.; Reisner, E. Interfacing nature's catalytic machinery with synthetic materials for semi-artificial photosynthesis. *Nature Nanotechnology* **2018**, *13* (10), 890–899.
- (25) Van De Krol, R.; Grätzel, M. *Electronic Materials: Science and Technology, Introduction*; Springer US, 2012; pp 3–11.
- (26) Fang, X.; Kalathil, S.; Reisner, E. Semi-biological approaches to solar-to-chemical conversion. *Chemical Society Reviews* **2020**, *49* (14), 4926–4952.
- (27) Yau, M. C. M.; Hayes, M.; Kalathil, S. Biocatalytic conversion of sunlight and carbon dioxide to solar fuels and chemicals. *RSC Advances* **2022**, *12* (26), 16396–16411.
- (28) Appel, A. M.; Bercaw, J. E.; Bocarsly, A. B.; Dobbek, H.; Dubois, D. L.; Dupuis, M.; Ferry, J. G.; Fujita, E.; Hille, R.; Kenis, P. J. A.; et al. Frontiers, Opportunities, and Challenges in Biochemical and Chemical Catalysis of CO₂ Fixation. *Chemical Reviews* **2013**, *113* (8), 6621–6658.
- (29) Armstrong, F. A.; Hirst, J. Reversibility and efficiency in electrocatalytic energy conversion and lessons from enzymes. *Proceedings of the National Academy of Sciences* **2011**, *108* (34), 14049–14054.
- (30) Sokol, K. P.; Robinson, W. E.; Oliveira, A. R.; Warnan, J.; Nowaczyk, M. M.; Ruff, A.; Pereira, I. A. C.; Reisner, E. Photoreduction of CO₂ with a Formate Dehydrogenase Driven by Photosystem II Using a Semi-artificial Z-Scheme Architecture. *J. Am. Chem. Soc.* **2018**, *140* (48), 16418–16422.
- (31) Xiao, K.; Liang, J.; Wang, X.; Hou, T.; Ren, X.; Yin, P.; Ma, Z.; Zeng, C.; Gao, X.; Yu, T.; et al. Panoramic insights into semi-artificial photosynthesis: origin, development, and future perspective. *Energy & Environmental Science* **2022**, *15* (2), 529–549.
- (32) Lovley, D. R. Electrotrophy: Other microbial species, iron, and electrodes as electron donors for microbial respirations. *Bioresour. Technol.* **2022**, *345*, No. 126553.
- (33) Yang, P. Liquid Sunlight: The Evolution of Photosynthetic Biohybrids. *Nano Letters* **2021**, *21* (13), 5453–5456.
- (34) Krasnovsky, A. A.; Nikandrov, V. V. The photobiocatalytic system: Inorganic semiconductors coupled to bacterial cells. *FEBS Lett.* **1987**, *219* (1), 93–96.
- (35) MARUTHAMUTHU, P.; MUTHU, S.; GURUNATHAN, K.; ASHOKKUMAR, M.; SASTRI, M. Photobiocatalysis: hydrogen evolution using a semiconductor coupled with photosynthetic bacteria. *Int. J. Hydrogen Energy* **1992**, *17* (11), 863.
- (36) Gurnathan, K. Photobiocatalytic production of hydrogen using sensitized TiO₂–MV²⁺ system coupled *Rhodospseudomonas capsulata*. *Journal of Molecular Catalysis A: Chemical* **2000**, *156* (1–2), 59–67.
- (37) Pontrelli, S.; Chiu, T.-Y.; Lan, E. I.; Chen, F. Y. H.; Chang, P.; Liao, J. C. *Escherichia coli* as a host for metabolic engineering. *Metabolic Engineering* **2018**, *50*, 16–46.
- (38) Honda, Y.; Hagiwara, H.; Ida, S.; Ishihara, T. Application to Photocatalytic H₂ Production of a Whole-Cell Reaction by Recombinant *Escherichia coli* Cells Expressing [FeFe]-Hydrogenase and Maturase Genes. *Angew. Chem.* **2016**, *128* (28), 8177–8180.
- (39) Wang, B.; Zeng, C.; Chu, K. H.; Wu, D.; Yip, H. Y.; Ye, L.; Wong, P. K. Enhanced Biological Hydrogen Production from *Escherichia coli* with Surface Precipitated Cadmium Sulfide Nanoparticles. *Advanced Energy Materials* **2017**, *7* (20), No. 1700611.
- (40) Wei, W.; Sun, P.; Li, Z.; Song, K.; Su, W.; Wang, B.; Liu, Y.; Zhao, J. A surface-display biohybrid approach to light-driven hydrogen production in air. *Science Advances* **2018**, *4*, na.

- (41) Sakimoto, K. K.; Kornienko, N.; Yang, P. Cyborgian Material Design for Solar Fuel Production: The Emerging Photosynthetic Biohybrid Systems. *Acc. Chem. Res.* **2017**, *50* (3), 476–481.
- (42) Kuhl, K. P.; Cave, E. R.; Abram, D. N.; Jaramillo, T. F. New insights into the electrochemical reduction of carbon dioxide on metallic copper surfaces. *Energy & Environmental Science* **2012**, *5* (5), 7050.
- (43) Thauer, R. K.; Kaster, A.-K.; Seedorf, H.; Buckel, W.; Hedderich, R. Methanogenic archaea: ecologically relevant differences in energy conservation. *Nature Reviews Microbiology* **2008**, *6* (8), 579–591.
- (44) Ye, J.; Yu, J.; Zhang, Y.; Chen, M.; Liu, X.; Zhou, S.; He, Z. Light-driven carbon dioxide reduction to methane by *Methanosarcina barkeri*-CdS biohybrid. *Applied Catalysis B: Environmental* **2019**, *257*, 117916.
- (45) Larkum, A. W. Limitations and prospects of natural photosynthesis for bioenergy production. *Curr Opin Biotechnol* **2010**, *21* (3), 271–276.
- (46) Sakimoto, K. K.; Zhang, S. J.; Yang, P. Cysteine–Cystine Photoregeneration for Oxygenic Photosynthesis of Acetic Acid from CO₂ by a Tandem Inorganic–Biological Hybrid System. *Nano Letters* **2016**, *16* (9), 5883–5887.
- (47) Zhang, H.; Liu, H.; Tian, Z.; Lu, D.; Yu, Y.; Cestellos-Blanco, S.; Sakimoto, K. K.; Yang, P. Bacteria photosensitized by intracellular gold nanoclusters for solar fuel production. *Nature Nanotechnology* **2018**, *13* (10), 900–905.
- (48) Wang, B.; Jiang, Z.; Yu, J. C.; Wang, J.; Wong, P. K. Enhanced CO₂ reduction and valuable C₂₊ chemical production by a CdS-photosynthetic hybrid system. *Nanoscale* **2019**, *11* (19), 9296–9301.
- (49) Chen, M.; Zhou, X. F.; Yu, Y. Q.; Liu, X.; Zeng, R. J.; Zhou, S. G.; He, Z. Light-driven nitrous oxide production via autotrophic denitrification by self-photosensitized *Thiobacillus denitrificans*. *Environ Int* **2019**, *127*, 353–360.
- (50) Gai, P.; Yu, W.; Zhao, H.; Qi, R.; Li, F.; Liu, L.; Lv, F.; Wang, S. Solar-Powered Organic Semiconductor–Bacteria Biohybrids for CO₂ Reduction into Acetic Acid. *Angewandte Chemie International Edition* **2020**, *59* (18), 7224–7229.
- (51) Park, J. H.; Lee, S. H.; Cha, G. S.; Choi, D. S.; Nam, D. H.; Lee, J. H.; Lee, J.-K.; Yun, C.-H.; Jeong, K. J.; Park, C. B. Cofactor-Free Light-Driven Whole-Cell Cytochrome P450 Catalysis. *Angew. Chem.* **2015**, *127* (3), 983–987.
- (52) Tran, N.-H.; Nguyen, D.; Dwaraknath, S.; Mahadevan, S.; Chavez, G.; Nguyen, A.; Dao, T.; Mullen, S.; Nguyen, T.-A.; Cheruzel, L. E. An Efficient Light-Driven P450 BM3 Biocatalyst. *J. Am. Chem. Soc.* **2013**, *135* (39), 14484–14487.
- (53) Rowe, S. F.; Le Gall, G.; Ainsworth, E. V.; Davies, J. A.; Lockwood, C. W. J.; Shi, L.; Elliston, A.; Roberts, I. N.; Waldron, K. W.; Richardson, D. J.; et al. Light-Driven H₂ Evolution and C≡C or C=O Bond Hydrogenation by *Shewanella oneidensis*: A Versatile Strategy for Photocatalysis by Nonphotosynthetic Microorganisms. *ACS Catalysis* **2017**, *7* (11), 7558–7566.
- (54) Edwards, E. H.; Jelušić, J.; Kosko, R. M.; McClelland, K. P.; Ngarnim, S. S.; Chiang, W.; Lampa-Pastirk, S.; Krauss, T. D.; Bren, K. L. *Shewanella oneidensis* MR-1 respire CdSe quantum dots for photocatalytic hydrogen evolution. *Proceedings of the National Academy of Sciences* **2023**, *120* (17), na DOI: 10.1073/pnas.2206975120.
- (55) Chen, X.; Lawrence, J. M.; Wey, L. T.; Schertel, L.; Jing, Q.; Vignolini, S.; Howe, C. J.; Kar-Narayan, S.; Zhang, J. Z. 3D-printed hierarchical pillar array electrodes for high-performance semi-artificial photosynthesis. *Nat. Mater.* **2022**, *21* (7), 811–818.
- (56) Wang, Q.; Kalathil, S.; Pornrungroj, C.; Sahm, C. D.; Reisner, E. Bacteria–photocatalyst sheet for sustainable carbon dioxide utilization. *Nature Catalysis* **2022**, *5* (7), 633–641.
- (57) Rabaey, K.; Rozendal, R. A. Microbial electrosynthesis — revisiting the electrical route for microbial production. *Nature Reviews Microbiology* **2010**, *8* (10), 706–716.
- (58) Zhang, J. Z.; Bombelli, P.; Sokol, K. P.; Fantuzzi, A.; Rutherford, A. W.; Howe, C. J.; Reisner, E. Photoelectrochemistry of Photosystem II in Vitro vs in Vivo. *J. Am. Chem. Soc.* **2018**, *140* (1), 6–9.
- (59) Wenzel, T.; Härtter, D.; Bombelli, P.; Howe, C. J.; Steiner, U. Porous translucent electrodes enhance current generation from photosynthetic biofilms. *Nature Communications* **2018**, *9* (1), na DOI: 10.1038/s41467-018-03320-x.
- (60) Zhang, J. Z.; Sokol, K. P.; Paul, N.; Romero, E.; Van Grondelle, R.; Reisner, E. Competing charge transfer pathways at the photosystem II–electrode interface. *Nature Chemical Biology* **2016**, *12* (12), 1046–1052.
- (61) McCormick, A. J.; Bombelli, P.; Bradley, R. W.; Thorne, R.; Wenzel, T.; Howe, C. J. Biophotovoltaics: oxygenic photosynthetic organisms in the world of bioelectrochemical systems. *Energy & Environmental Science* **2015**, *8* (4), 1092–1109.
- (62) Liu, C.; Gallagher, J. J.; Sakimoto, K. K.; Nichols, E. M.; Chang, C. J.; Chang, M. C. Y.; Yang, P. Nanowire–Bacteria Hybrids for Unassisted Solar Carbon Dioxide Fixation to Value-Added Chemicals. *Nano Letters* **2015**, *15* (5), 3634–3639.
- (63) Qian, F.; Wang, H.; Ling, Y.; Wang, G.; Thelen, M. P.; Li, Y. Photoenhanced Electrochemical Interaction between *Shewanella* and a Hematite Nanowire Photoanode. *Nano Letters* **2014**, *14* (6), 3688–3693.
- (64) Su, Y.; Cestellos-Blanco, S.; Kim, J. M.; Shen, Y.-X.; Kong, Q.; Lu, D.; Liu, C.; Zhang, H.; Cao, Y.; Yang, P. Close-Packed Nanowire-Bacteria Hybrids for Efficient Solar-Driven CO₂ Fixation. *Joule* **2020**, *4* (4), 800–811.
- (65) Cestellos-Blanco, S.; Zhang, H.; Kim, J. M.; Shen, Y.-X.; Yang, P. Photosynthetic semiconductor biohybrids for solar-driven biocatalysis. *Nature Catalysis* **2020**, *3* (3), 245–255.
- (66) Li, S.; Cheng, C.; Thomas, A. Carbon-Based Microbial-Fuel-Cell Electrodes: From Conductive Supports to Active Catalysts. *Adv. Mater.* **2017**, *29* (8), No. 1602547.
- (67) Sakimoto, K. K.; Kornienko, N.; Cestellos-Blanco, S.; Lim, J.; Liu, C.; Yang, P. Physical Biology of the Materials–Microorganism Interface. *J. Am. Chem. Soc.* **2018**, *140* (6), 1978–1985.
- (68) Flexer, V.; Jourdin, L. Purposely Designed Hierarchical Porous Electrodes for High Rate Microbial Electrosynthesis of Acetate from Carbon Dioxide. *Acc. Chem. Res.* **2020**, *53* (2), 311–321.
- (69) Dogutan, D. K.; Nocera, D. G. Artificial Photosynthesis at Efficiencies Greatly Exceeding That of Natural Photosynthesis. *Acc. Chem. Res.* **2019**, *52* (11), 3143–3148.
- (70) Nocera, D. G. The Artificial Leaf. *Acc. Chem. Res.* **2012**, *45* (5), 767–776.
- (71) Haber, F.; Van Oordt, G. Über die Bildung von Ammoniak den Elementen. *Zeitschrift für anorganische Chemie* **1905**, *44* (1), 341–378.
- (72) Tamaru, K.; Jennings, J. *Catalytic Ammonia Synthesis*; Springer, 1991.
- (73) Schlögl, R. Ammonia synthesis. *Handbook of heterogeneous catalysis*; Wiley-VCH, 2008; pp 2501–2575.
- (74) Schlögl, R. *Handbook of heterogeneous catalysis*; Wiley, 2008; Vol. 5, pp 2501–2575.
- (75) Smil, V. Detonator of the population explosion. *Nature* **1999**, *400* (6743), 415.
- (76) Qin, Q.; Oschatz, M. Overcoming Chemical Inertness under Ambient Conditions: A Critical View on Recent Developments in Ammonia Synthesis via Electrochemical N₂ Reduction by Asking Five Questions. *ChemElectroChem* **2020**, *7* (4), 878–889.
- (77) Wang, B.; Xiao, K.; Jiang, Z.; Wang, J.; Yu, J. C.; Wong, P. K. Biohybrid photoheterotrophic metabolism for significant enhancement of biological nitrogen fixation in pure microbial cultures. *Energy & Environmental Science* **2019**, *12* (7), 2185–2191.
- (78) Lu, S.; Guan, X.; Liu, C. Electricity-powered artificial root nodule. *Nature Communications* **2020**, *11* (1), na DOI: 10.1038/s41467-020-15314-9.
- (79) Liu, C.; Sakimoto, K. K.; Colón, B. C.; Silver, P. A.; Nocera, D. G. Ambient nitrogen reduction cycle using a hybrid inorganic–biological system. *Proceedings of the National Academy of Sciences* **2017**, *114* (25), 6450–6455.

- (80) Sherbo, R. S.; Silver, P. A.; Nocera, D. G. Riboflavin synthesis from gaseous nitrogen and carbon dioxide by a hybrid inorganic-biological system. *Proceedings of the National Academy of Sciences* **2022**, 119 (37), na DOI: 10.1073/pnas.2210538119.
- (81) Segev, G.; Kibsgaard, J.; Hahn, C.; Xu, Z. J.; Cheng, W.-H.; Deutsch, T. G.; Xiang, C.; Zhang, J. Z.; Hammarström, L.; Nocera, D. G.; et al. The 2022 solar fuels roadmap. *Journal of Physics D: Applied Physics* **2022**, 55 (32), No. 323003.
- (82) Gilliland, G. D. Photoluminescence spectroscopy of crystalline semiconductors. *Materials Science and Engineering: R: Reports* **1997**, 18 (3–6), 99.
- (83) Shen, H.; Wang, Y.-Z.; Liu, G.; Li, L.; Xia, R.; Luo, B.; Wang, J.; Suo, D.; Shi, W.; Yong, Y.-C. A Whole-Cell Inorganic-Biohybrid System Integrated by Reduced Graphene Oxide for Boosting Solar Hydrogen Production. *ACS Catalysis* **2020**, 10 (22), 13290–13295.
- (84) Luo, B.; Wang, Y. Z.; Li, D.; Shen, H.; Xu, L. X.; Fang, Z.; Xia, Z.; Ren, J.; Shi, W.; Yong, Y. C. A Periplasmic Photosensitized Biohybrid System for Solar Hydrogen Production. *Advanced Energy Materials* **2021**, 11 (19), No. 2100256.
- (85) Nie, C.; Ni, W.; Gong, L.; Jiang, J.; Wang, J.; Wang, M. Charge transfer dynamics and catalytic performance of a covalently linked hybrid assembly comprising a functionalized cobalt tetraazamacrocyclic catalyst and CuInS₂/ZnS quantum dots for photochemical hydrogen production. *Journal of Materials Chemistry A* **2019**, 7 (48), 27432–27440.
- (86) Guan, X.; Ersan, S.; Hu, X.; Atallah, T. L.; Xie, Y.; Lu, S.; Cao, B.; Sun, J.; Wu, K.; Huang, Y.; et al. Maximizing light-driven CO(2) and N(2) fixation efficiency in quantum dot-bacteria hybrids. *Nat Catal* **2022**, 5 (11), 1019–1029.
- (87) Kornienko, N.; Sakimoto, K. K.; Herlihy, D. M.; Nguyen, S. C.; Alivisatos, A. P.; Harris, C. B.; Schwartzberg, A.; Yang, P. Spectroscopic elucidation of energy transfer in hybrid inorganic–biological organisms for solar-to-chemical production. *Proceedings of the National Academy of Sciences* **2016**, 113 (42), 11750–11755.
- (88) Berera, R.; Van Grondelle, R.; Kennis, J. T. M. Ultrafast transient absorption spectroscopy: principles and application to photosynthetic systems. *Photosynthesis Research* **2009**, 101 (2–3), 105–118.
- (89) Knowles, K. E.; Koch, M. D.; Shelton, J. L. Three applications of ultrafast transient absorption spectroscopy of semiconductor thin films: spectroelectrochemistry, microscopy, and identification of thermal contributions. *Journal of Materials Chemistry C* **2018**, 6 (44), 11853–11867.
- (90) Kambhampati, P. Unraveling the structure and dynamics of excitons in semiconductor quantum dots. *Accounts of chemical research* **2011**, 44 (1), 1–13.
- (91) Utterback, J. K.; Wilker, M. B.; Brown, K. A.; King, P. W.; Eaves, J. D.; Dukovic, G. Competition between electron transfer, trapping, and recombination in CdS nanorod–hydrogenase complexes. *Phys. Chem. Chem. Phys.* **2015**, 17 (8), 5538–5542.
- (92) Baikie, T. K.; Wey, L. T.; Lawrence, J. M.; Medipally, H.; Reisner, E.; Nowaczyk, M. M.; Friend, R. H.; Howe, C. J.; Schnedermann, C.; Rao, A.; et al. Photosynthesis re-wired on the pico-second timescale. *Nature* **2023**, 615 (7954), 836–840.
- (93) Munson, K. T.; Kennehan, E. R.; Asbury, J. B. Structural origins of the electronic properties of materials via time-resolved infrared spectroscopy. *Journal of Materials Chemistry C* **2019**, 7 (20), 5889–5909.
- (94) Mezzetti, A.; Leibl, W. Time-resolved infrared spectroscopy in the study of photosynthetic systems. *Photosynthesis Research* **2017**, 131 (2), 121–144.
- (95) Striplin, D.; Crosby, G. Photophysical investigations of rhenium (I) Cl (CO) 3 (phenanthroline) complexes. *Coord. Chem. Rev.* **2001**, 211 (1), 163–175.
- (96) Striplin, D.; Crosby, G. Nature of the emitting 3MLCT manifold of rhenium (I)(diimine)(CO) 3Cl complexes. *Chemical physics letters* **1994**, 221 (5–6), 426–430.
- (97) Hawecker, J.; Lehn, J. M.; Ziessel, R. Photochemical and Electrochemical Reduction of Carbon Dioxide to Carbon Monoxide Mediated by (2,2′-Bipyridine)tricarboxylchlororhenium(I) and Related Complexes as Homogeneous Catalysts. *Helv. Chim. Acta* **1986**, 69 (8), 1990–2012.
- (98) Blanco-Rodríguez, A. M.; Busby, M.; Gradinaru, C.; Crane, B. R.; Di Bilio, A. J.; Matousek, P.; Towrie, M.; Leigh, B. S.; Richards, J. H.; Vlcek, A.; Gray, H. B. Excited-State Dynamics of Structurally Characterized [Re(CO)₃(phen)(HisX)]⁺ (X) 83, 109 Pseudomonas aeruginosa Azurins in Aqueous Solution. *J. Am. Chem. Soc.* **2006**, 128, 4365–4370.
- (99) Fujita, E.; Grills, D. C.; Manbeck, G. F.; Polyansky, D. E. Understanding the Role of Inter- and Intramolecular Promoters in Electro- and Photochemical CO₂ Reduction Using Mn, Re, and Ru Catalysts. *Acc. Chem. Res.* **2022**, 55 (5), 616–628.
- (100) Riplinger, C.; Carter, E. A. Influence of Weak Brønsted Acids on Electrocatalytic CO₂ Reduction by Manganese and Rhenium Bipyridine Catalysts. *ACS Catalysis* **2015**, 5 (2), 900–908.
- (101) Riplinger, C.; Sampson, M. D.; Ritzmann, A. M.; Kubiak, C. P.; Carter, E. A. Mechanistic Contrasts between Manganese and Rhenium Bipyridine Electrocatalysts for the Reduction of Carbon Dioxide. *J. Am. Chem. Soc.* **2014**, 136 (46), 16285–16298.
- (102) Takematsu, K.; Williamson, H.; Blanco-Rodríguez, A. M.; Sokolová, L.; Nikolovski, P.; Kaiser, J. T.; Towrie, M.; Clark, I. P.; Vlček, A.; Winkler, J. R.; et al. Tryptophan-Accelerated Electron Flow Across a Protein–Protein Interface. *J. Am. Chem. Soc.* **2013**, 135 (41), 15515–15525.
- (103) Keane, P. M.; O’Sullivan, K.; Poynton, F. E.; Poulsen, B. C.; Sazanovich, I. V.; Towrie, M.; Cardin, C. J.; Sun, X.-Z.; George, M. W.; Gunnlaugsson, T.; et al. Understanding the factors controlling the photo-oxidation of natural DNA by enantiomerically pure intercalating ruthenium polypyridyl complexes through TA/TRIR studies with polydeoxynucleotides and mixed sequence oligodeoxynucleotides. *Chemical Science* **2020**, 11 (32), 8600–8609.
- (104) Ryan, D. E.; Hartl, F. IR Spectro-electrochemistry and Group-6 a-diimine Catalysts of CO₂ Reduction. *Electrochemical Reduction of Carbon Dioxide: Overcoming the Limitations of Photosynthesis* **2018**, 21, 182.
- (105) Taylor, J. O.; Veenstra, F. L. P.; Chippindale, A. M.; Calhorda, M. J.; Hartl, F. Group 6 Metal Complexes as Electrocatalysts of CO₂ Reduction: Strong Substituent Control of the Reduction Path of [Mo(η^3 -allyl)(CO)₂(x,x′-dimethyl-2,2′-bipyridine)(NCS)] (x = 4–6). *Organometallics* **2019**, 38 (6), 1372–1390.
- (106) Ashley, K. SOLUTION INFRARED SPECTROELECTRO-CHEMISTRY: A REVIEW. *Talanta* **1991**, 38 (11), 1209–1218.
- (107) Wang, H.; Zhou, Y.-W.; Cai, W.-B. Recent applications of in situ ATR-IR spectroscopy in interfacial electrochemistry. *Current Opinion in Electrochemistry* **2017**, 1 (1), 73–79.
- (108) Mojet, B. L.; Ebbesen, S. D.; Lefferts, L. Light at the interface: the potential of attenuated total reflection infrared spectroscopy for understanding heterogeneous catalysis in water. *Chemical Society Reviews* **2010**, 39 (12), 4643.
- (109) Parikh, S. J.; Mukome, F. N. D.; Zhang, X. ATR–FTIR spectroscopic evidence for biomolecular phosphorus and carboxyl groups facilitating bacterial adhesion to iron oxides. *Colloids and Surfaces B: Biointerfaces* **2014**, 119, 38–46.
- (110) Kang, S.-Y.; Bremer, P. J.; Kim, K.-W.; McQuillan, A. J. Monitoring Metal Ion Binding in Single-Layer Pseudomonas aeruginosa Biofilms Using ATR–IR Spectroscopy. *Langmuir* **2006**, 22 (1), 286–291.
- (111) Upritchard, H. G.; Yang, J.; Bremer, P. J.; Lamont, I. L.; McQuillan, A. J. Adsorption to Metal Oxides of the Pseudomonas aeruginosa Siderophore Pyoverdine and Implications for Bacterial Biofilm Formation on Metals. *Langmuir* **2007**, 23 (13), 7189–7195.
- (112) Mulvaney, S. P.; Keating, C. D. Raman Spectroscopy. *Anal. Chem.* **2000**, 72 (12), 145–158.
- (113) Chen, Z.; Zhang, H.; Guo, P.; Zhang, J.; Tira, G.; Kim, Y. J.; Wu, Y. A.; Liu, Y.; Wen, J.; Rajh, T.; et al. Semi-artificial Photosynthetic CO₂ Reduction through Purple Membrane Re-engineering with Semiconductor. *J. Am. Chem. Soc.* **2019**, 141 (30), 11811–11815.

- (114) Ye, J.; Ren, G.; Kang, L.; Zhang, Y.; Liu, X.; Zhou, S.; He, Z. Efficient Photoelectron Capture by Ni Decoration in Methanosarcina barkeri-CdS Biohybrids for Enhanced Photocatalytic CO₂-to-CH₄ Conversion. *iScience* **2020**, 23 (7), No. 101287.
- (115) Yi, Z.; Tian, S.; Geng, W.; Zhang, T.; Zhang, W.; Huang, Y.; Barad, H. N.; Tian, G.; Yang, X. Y. A Semiconductor Biohybrid System for Photo-Synergetic Enhancement of Biological Hydrogen Production. *Chemistry – A European Journal* **2023**, 29 (18), na.
- (116) Yano, J.; Yachandra, V. K. X-ray absorption spectroscopy. *Photosynthesis Research* **2009**, 102 (2–3), 241–254.
- (117) Lewerenz, H.-J.; Lichterman, M. F.; Richter, M. H.; Crumlin, E. J.; Hu, S.; Axnanda, S.; Favaro, M.; Drisdell, W.; Hussain, Z.; Brunswig, B. S.; et al. Operando Analyses of Solar Fuels Light Absorbers and Catalysts. *Electrochim. Acta* **2016**, 211, 711–719.
- (118) Smolentsev, G.; Sundström, V. Time-resolved X-ray absorption spectroscopy for the study of molecular systems relevant for artificial photosynthesis. *Coord. Chem. Rev.* **2015**, 304–305, 117–132.
- (119) Sanchez Casalongue, H. G.; Ng, M. L.; Kaya, S.; Friebe, D.; Ogasawara, H.; Nilsson, A. In Situ Observation of Surface Species on Iridium Oxide Nanoparticles during the Oxygen Evolution Reaction. *Angewandte Chemie International Edition* **2014**, 53 (28), 7169–7172.
- (120) van der Mei, H. C.; de Vries, J.; Busscher, H. J. X-ray photoelectron spectroscopy for the study of microbial cell surfaces. *Surface Science Reports* **2000**, 39 (1), 1–24.
- (121) Liu, J.; Guo, X.; He, L.; Jiang, L.-P.; Zhou, Y.; Zhu, J.-J. Enhanced photocatalytic CO₂ reduction on biomineralized CdS via an electron conduit in bacteria. *Nanoscale* **2023**, 15 (25), 10755–10762.
- (122) Martins, M.; Toste, C.; Pereira, I. A. Enhanced light-driven hydrogen production by self-photosensitized biohybrid systems. *Angewandte Chemie International Edition* **2021**, 60 (16), 9055–9062.
- (123) Zhou, X.; Zeng, Y.; Lv, F.; Bai, H.; Wang, S. Organic Semiconductor–Organism Interfaces for Augmenting Natural and Artificial Photosynthesis. *Acc. Chem. Res.* **2022**, 55 (2), 156–170.
- (124) He, Y.; Wang, S.; Han, X.; Shen, J.; Lu, Y.; Zhao, J.; Shen, C.; Qiao, L. Photosynthesis of Acetate by *Sporomusa ovata* – CdS Biohybrid System. *ACS Applied Materials & Interfaces* **2022**, 14 (20), 23364–23374.
- (125) Wang, Z.; Gao, D.; Zhan, Y.; Xing, C. Enhancing the Light Coverage of Photosynthetic Bacteria to Augment Photosynthesis by Conjugated Polymer Nanoparticles. *ACS Appl Bio Mater* **2020**, 3 (5), 3423–3429.
- (126) Zhang, H.; Catania, R.; Jeuken, L. J. C. Membrane Protein Modified Electrodes in Bioelectrocatalysis. *Catalysts* **2020**, 10 (12), 1427.
- (127) Weliwatte, N. S.; Grattieri, M.; Minter, S. D. Rational design of artificial redox-mediating systems toward upgrading photo-bioelectrocatalysis. *Photochemical & Photobiological Sciences* **2021**, 20 (10), 1333–1356.
- (128) Kato, M.; Zhang, J. Z.; Paul, N.; Reisner, E. Protein film photoelectrochemistry of the water oxidation enzyme photosystem II. *Chem. Soc. Rev.* **2014**, 43 (18), 6485–6497.
- (129) Hasan, K.; Bekir Yildiz, H.; Sperling, E.; Ó Conghaile, P.; Packer, M. A.; Leech, D.; Hägerhäll, C.; Gorton, L. Photo-electrochemical communication between cyanobacteria (*Leptolyngbia* sp.) and osmium redox polymer modified electrodes. *Phys. Chem. Chem. Phys.* **2014**, 16 (45), 24676–24680.
- (130) Nawrocki, W. J.; Jones, M. R.; Frese, R. N.; Croce, R.; Friebe, V. M. In situ time-resolved spectroelectrochemistry reveals limitations of biohybrid photoelectrode performance. *Joule* **2023**, 7 (3), 529–544.
- (131) Cestellos-Blanco, S.; Chan, R. R.; Shen, Y.-X.; Kim, J. M.; Tacke, T. A.; Ledbetter, R.; Yu, S.; Seefeldt, L. C.; Yang, P. Photosynthetic biohybrid coculture for tandem and tunable CO₂ and N₂ fixation. *Proceedings of the National Academy of Sciences* **2022**, 119 (26), na DOI: 10.1073/pnas.2122364119.
- (132) Kim, J.; Cestellos-Blanco, S.; Shen, Y.-X.; Cai, R.; Yang, P. Enhancing Biohybrid CO₂ to Multicarbon Reduction via Adapted Whole-Cell Catalysts. *Nano Letters* **2022**, 22 (13), 5503–5509.
- (133) Fang, X.; Kalathil, S.; Divitini, G.; Wang, Q.; Reisner, E. A three-dimensional hybrid electrode with electroactive microbes for efficient electrogenesis and chemical synthesis. *Proceedings of the National Academy of Sciences* **2020**, 117 (9), 5074–5080.
- (134) Bond, D. R.; Lovley, D. R. Electricity Production by *Geobacter sulfurreducens* Attached to Electrodes. *Appl. Environ. Microbiol.* **2003**, 69 (3), 1548–1555.
- (135) Kalathil, S.; Patil, S. A.; Pant, D. Microbial Fuel Cells: Electrode Materials. *Encyclopedia of Interfacial Chemistry* **2018**, 309–318.
- (136) Lovley, D. R.; Walker, D. J. F. *Geobacter* Protein Nanowires. *Front Microbiol* **2019**, 10, 2078.
- (137) Yi, H.; Nevin, K. P.; Kim, B. C.; Franks, A. E.; Klimes, A.; Tender, L. M.; Lovley, D. R. Selection of a variant of *Geobacter sulfurreducens* with enhanced capacity for current production in microbial fuel cells. *Biosens Bioelectron* **2009**, 24 (12), 3498–3503.
- (138) Malvankar, N. S.; Vargas, M.; Nevin, K. P.; Franks, A. E.; Leang, C.; Kim, B. C.; Inoue, K.; Mester, T.; Covalla, S. F.; Johnson, J. P.; et al. Tunable metallic-like conductivity in microbial nanowire networks. *Nat Nanotechnol* **2011**, 6 (9), 573–579.
- (139) Ueki, T.; Nevin, K. P.; Woodard, T. L.; Lovley, D. R. Converting carbon dioxide to butyrate with an engineered strain of *Clostridium ljungdahlii*. *mBio* **2014**, 5 (5), e01636–01614.
- (140) Zhang, R.; He, Y.; Yi, J.; Zhang, L.; Shen, C.; Liu, S.; Liu, L.; Liu, B.; Qiao, L. Proteomic and Metabolic Elucidation of Solar-Powered Biomanufacturing by Bio-Abiotic Hybrid System. *Chem* **2020**, 6 (1), 234–249.
- (141) Kanan, M. W.; Surendranath, Y.; Nocera, D. G. Cobalt–phosphate oxygen-evolving compound. *Chem. Soc. Rev.* **2009**, 38 (1), 109–114.